# Computational Modeling of Cervical Remodeling During Pre-term Labor

Thesis

Presented in partial fulfillment of the requirements for graduation *with honors research distinction* in Biomedical Engineering in the undergraduate colleges of The Ohio State University

By

Cory Stein

Undergraduate Program in Engineering

The Ohio State University

2017

Thesis Committee:

Dr. Samir Ghadiali, Advisor

Abstract

Pre-term labor (PTL) is the leading cause of death for neonates and is on the rise in industrial nations. If it does not cause death, there is a greater chance that physical or intellectual abilities can occur. Normally, the cervix stays closed and firm during the gestation period to keep the baby in a controlled environment and will remodel as labor begins. The cervix goes through two phases, called cervical softening and cervical ripening, that cause the cervix to remodel. Issues in these remodeling phases can lead to PTL. PTL occurs when labor is initiated early in the gestation period, causing pre-mature effacement and dilation of the cervix. Some currently known factors for PTL are cervical remodeling, pro-inflammatory cytokine or fibronectin presence in combination with cervical length, a shortened cervix, and the patient previously going through PTL. Finally, the cervical mucus plug (CMP) is an important feature of the female reproductive environment. This is a viscoelastic material that acts a block to bacteria from entering the cervix. The biophysical properties of the CMP could act as biomarkers for PTL.

The goal of this undergraduate research project was to develop a sophisticated computational model that simulates cervical remodeling during PTL and to use this model to investigate how changes in cervical tissue and CMP biophysical properties influence PTL. All factors that make a woman at risk for PTL are not completely understood and efforts are still being made to see what doctors can monitor to try and prevent PTL. Additionally, the role of the CMP in cervical remodeling was investigated and seen if it could be central in preventing PTL. The CMP has not been modeled with

the cervix before and is a unique part of the project. A few hypotheses were made during the project, two of which were that alterations in the cervical tissue and the CMP biophysical properties would change the opening of the cervix. Another one made was that the model would support that cervical length has a large influence on cervical opening. Finally the main hypothesis made was the CMP as an overall structure is critical in regulating cervical opening. For the cervical tissue, Poisson's Ratio, Young's Modulus, and force were looked at. For the CMP, density, viscosity, and surface tension were tested.

After computations, it was found that the Young's Modulus and force were important factors in preventing PTL for the cervical tissue. The Young's Modulus in the circumferential direction especially was significant in keeping the cervix from opening. This supported the hypothesis that the cervical tissue properties will play a role in preventing PTL. The viscosity of the CMP started to have an influence on the system at high values. The surface tension may have played a greater role in preventing PTL if there were not limitations in the model. The CMP could not slip along the fluid structure interaction boundary and this could have altered how the properties affected cervical opening. As a result, it was questionable whether these were noteworthy so it did not support the hypothesis that the biophysical properties of the CMP would cause changes to the cervical opening. Similarly, the CMP as a whole did not have a large influence on the preventing PTL, so it proved the main hypothesis that it would to be false. Finally, cervical length was tested and showed that a short cervix is more susceptible to cervical opening. This supported the last hypothesis that the model would verify that cervical

length is important. From the cervical length studies, it was also found that the CMP started to have a greater influence with a shorter cervix. This should be kept in mind when proceeding with future steps in the project.

An improvement for the project would be to find a way to have the points of the CMP on the fluid structure interface to slip. If this occurred, the results of the properties may have changed. One outlook would be to allow the cervical tissue to efface as well as dilate. Another outlook would be to create a more advanced model that includes the uterus. With the uterus, a pressure could be applied on the inside boundaries like the baby would. This would replace the force that is currently used and would be more anatomically accurate. A final outlook would be to change the viscosity of the CMP from Newtonian to a non-Newtonian shear thinning fluid. The viscosity is a non-linear fluid and the shear dependence of it may be vital in cervical opening and preventing PTL.

Acknowledgments

I would like to acknowledge Dr. Samir Ghadiali, my project advisor, for supporting me through the whole process of creating my project and collecting data. He was very helpful in teaching me how to use COMSOL and how to approach a research problem and attempt to find the solution. I would also like to acknowledge Dr. Jennifer Leight for sitting on my committee for my thesis defense. Finally, I would like to acknowledge Dr. Ghadiali's lab for providing insight into my project and helping me to have a better presentation.

Vita

June 2013 .....Ottawa Hills High School

June to July 2015……Study abroad program at Charles University, Prague

June to August 2016.....Intern at International Biomedical

Fields of Study

Major Field: Biomedical Engineering

Table of Contents

Abstract ..... ii

Acknowledgments ..... v

Vita ..... vi

CHAPTER 1: INTRODUCTION ..... 1

2.1: General methods and schematics ..... 8

2.2: Axial Symmetric Cylindrical Computational Model ..... 9

CHAPTER 3: RESULTS AND DISCUSSION ..... 27

CHAPTER 4: CONCLUSION ..... 50

REFERENCES ..... 54

List of Tables

Table 1: CMP Baseline Values ..... 12

Table 2: Cervical Tissue Baseline Values ..... 12

List of Figures

Figure 1: Effacement and dilation of the cervix. Effacement causes the cervix to become shorter, matching the width of the womb. Dilation then causes the cervix to open in order to create a channel for the baby to leave the body from. ("Cervical Dilation | Pregnancy Delivery | labor and Child Delivery :: Mothersspace," n.d.) ..... 2

Figure 2: Difference in cervical length. The first image seen is the normal cervical size, while the second image is a short cervix. Having a short cervix is a large indicator that someone will enter PTL. ("Short_cerix.jpg (301×225)," n.d.) ..... 5

Figure 3: Cervical mucus plug. This is an image of the plug outside of the body. It has viscoelastic properties, with both solid and liquid characteristics. (Becher et al., 2009) ... 6

Figure 4: General anatomical picture of the cervix. The first image shows an overview of the cervix, womb, and vagina. The second image shows what the cervix looks like when observed from below. (RN, n.d.) ..... 9

Figure 5: Schematic of the cervix. This is a representation of what will be modeled when testing the biophysical properties. The main areas focused on will be the cervical tissue and the CMP and their interactions..... 9

Figure 6: Axial symmetric cylindrical computational model. The R-axis is the horizontal axis, the Z-axis is the vertical axis, and the PHI-axis is the axis that the model rotates around. ..... 10

Figure 7: 3-Dimensional revolution of the axial symmetric model. This is what the model looks like when the axial symmetric conditions are incorporated. The conditions act on all the boundaries uniformly to get the results..... 11

Figure 8: Cervical tissue boundary conditions. These govern how the cervical tissue will operate when the model is run. ..... 14

Figure 9: CMP boundary conditions. These govern how the CMP will operate when the model is run. ..... 17

Figure 10: Moving mesh boundary conditions. These govern how the moving mesh will operate when the model is run. ..... 19

Figure 11: Fiber alignment of the cervical tissue in the orthotropic direction. These govern how the directional conditions will operate when the model is run. ..... 23

Figure 12: Mesh independent plot study. This models the degrees of freedom against percent cervical opening to determine the best mesh quality to use. ..... 27

Figure 13: 2-Dimensional view of von Mises stress on the cervical tissue. This shows the movement of the cervical tissue after the model was run. ..... 28

Figure 14: 3-Dimensional view of von Mises stress on the cervical tissue. This shows the movement of the cervical tissue after the model was run when the revolution of the material occurred. ..... 29

Figure 15: Cervical opening due to baseline changes in cervical tissue Poisson's Ratio. This plots shows the effect Poisson's Ratio has on PTL. ..... 30

Figure 16: Cervical opening due to baseline changes in cervical tissue force. This plots shows the effect force has on PTL. ..... 31

Figure 17: Cervical opening due to baseline changes in cervical tissue Young's Modulus. This plots shows the effect Young's Modulus has on PTL. ..... 32

Figure 18: 2-Dimensional view of the velocity of the CMP. This shows the movement of the fluid after the model was run. ..... 33
Figure 19: 3-Dimensional view of the velocity of the CMP. This shows the movement of the CMP after the model was run when the revolution of the material occurred. ..... 34
Figure 20: Cervical opening due to baseline change in CMP viscosity with varying Young's Modulus values. This plots shows the effect viscosity has on PTL. ..... 35
Figure 21: Cervical opening due to baseline change in CMP viscosity with varying force values. This plots shows the effect viscosity has on PTL. ..... 36
Figure 22: Cervical opening due to baseline change in CMP surface tension with varying Young's Modulus values. This plots shows the effect surface tension has on PTL. ..... 37
Figure 23: Cervical opening due to baseline change in CMP surface tension with varying force values. This plots shows the effect surface tension has on PTL. ..... 38
Figure 24: Points that should slip in model. This could alter the effect that surface tension has on the system. ..... 39
Figure 25: Model if points slipped. The CMP would be more stretched and the top and bottom boundaries would have greater tension values. ..... 40
Figure 26: Cervical opening due to baseline change in CMP density with varying Young's Modulus values. This plots shows the effect density has on PTL. ..... 41
Figure 27: Cervical opening due to baseline change in CMP density with varying force values. This plots shows the effect density has on PTL. ..... 42

Figure 28: Isotropic Sensitivity. This graph is showing the absolute value of the sensitivity for each parameter during the initial change from the baseline values. Young's Modulus and force can be seen to have the greatest significance in cervical opening. .... 43
Figure 29: Cervical opening due to changes in mean Young's Modulus. This shows the effect that the different directional forces have on percent opening in relation to each other. ..... 44
Figure 30: Cervical length study. This shows how different cervical lengths affect the percent opening of the cervix. ..... 46
Figure 31: Sensitivity comparison for a normal and short cervix. The short cervix sensitivities were closer for the cervical tissue and the CMP that indicates the CMP may play a larger role in preventing PTL. ..... 47
Figure 32: Cervical opening due to baseline changes in surface tension with a short cervix. The surface tension of the short cervix has a greater impact on cervical opening than the normal cervix. ..... 48
Figure 33: Cervical opening due to baseline changes in viscosity with a short cervix. The viscosity of the short cervix has a greater impact on cervical opening than the normal cervix..... 49
Figure 34: Cervix with the uterus included. This is a more anatomically accurate representation of the reproductive system and could produce improved results. ..... 53

# CHAPTER 1: INTRODUCTION

PTL is the leading causes of deaths for neonates and its rate has increased in most industrialized nations. (Goldenberg, Culhane, Iams, & Romero, 2008). Not only does it lead to death of the babies, but it can also cause intellectual or physical disorders, such as cerebral palsy (Huddy, Johnson, & Hope, 2001). Understanding the factors that can lead to PTL is imperative in reducing the death rates. If doctors are able to recognize the signs that a woman is at risk for PTL, they could take the necessary steps to protect the woman and her child. Establishing detailed history about the mother and her cervical environment could help to lead to more effective treatment and result in less cases of PTL.

Normally, the cervix stays closed and firm during the gestation period in order for the baby to have a controlled environment to grow (Kristin M. Myers, Hendon, et al., 2015). As a woman reaches term, the cervix begins to efface and dilate, as seen in Figure 1, in order to have a passage large enough for the baby to exit the body. Effacement is the shortening of the cervix as labor is initiated, while dilation is the opening of the cervix once effacement is almost complete. The cervix is usually able to stay closed until the end of gestation, but the early start of cervical opening, which has been hypothesized to be due to premature cervical remodeling, can cause PTL with babies less than 32 weeks of gestation at the high mortality risk (Kristin M. Myers, Hendon, et al., 2015). The causes of PTL are still under investigation, but they are all a result of cervical failure

(Kristin M. Myers, Hendon, et al., 2015). Recognizing the areas that the cervix is failing could lead to better treatment and reduce the mortality rates.

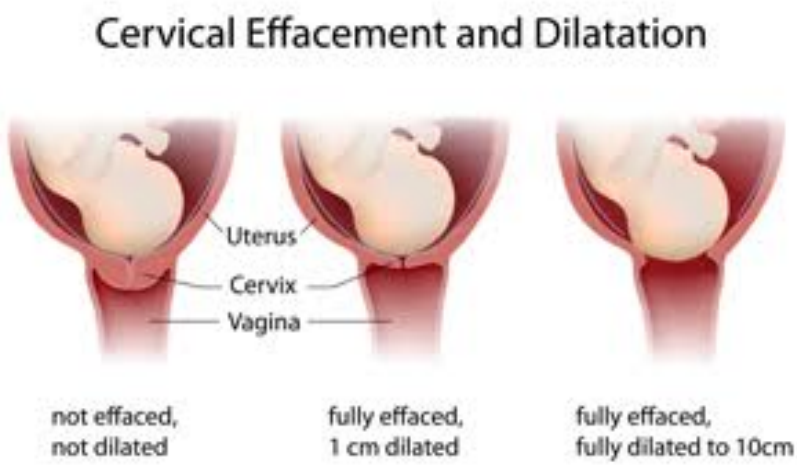


**Figure 1: Effacement and dilation of the cervix. Effacement causes the cervix to become shorter, matching the width of the womb. Dilation then causes the cervix to open in order to create a channel for the baby to leave the body from. ("Cervical Dilation | Pregnancy Delivery | labor and Child Delivery :: Mothersspace," n.d.)**

There are two main types of PTL, known as spontaneous and indicated (Mazaki-Tovi et al., 2007). Spontaneous PTL is when labor occurs with the membranes intact or if the membranes have ruptured (Mazaki-Tovi et al., 2007). Indicated PTL is when there are indications, either by the mother of the fetus, that require delivery before full term. In this case, the doctor will induce labor or perform a cesarean section to deliver the baby. One of the biggest risk factor for PTL is if a woman has had either spontaneous or indicated PTL in the past (Mazaki-Tovi et al., 2007). If a woman has entered PTL in the past, the doctor must pay extra attention to her since her risk is very high to go into PTL again with her next child (Mazaki-Tovi et al., 2007).

The cervix goes through two phases of remodeling once conception has occurred. The first is the cervix will slowly remodel itself through pregnancy, known as cervical softening (Kristin M. Myers, Feltovich, et al., 2015). Another phenomenon, called cervical ripening, then occurs close to delivery. Cervical ripening is the quicker shortening and softening of the cervix (Kristin M. Myers, Feltovich, et al., 2015). Problems can occur due to the extracellular matrix (ECM) remodeling incorrectly within the cervix (Kristin M. Myers, Feltovich, et al., 2015). Some factors that could cause the incorrect or premature remodeling could be patient age and mechanical loading of the ECM (Kristin M. Myers, Feltovich, et al., 2015). Other factors may come down to hormonal imbalance or inflammation of the ECM. Yet, the highest risk factor is still unknown and trying to be determined.

The presence of certain cytokines within the body can help to indicate if a woman is at risk for PTL. Pro-inflammatory cytokines in amniotic fluid, in combination with cervical length, are known predictors of PTL (Jung et al., 2016). The cytokines that are important in indicating intra-amniotic infection/inflammation are cervicovaginal interleukin (IL)-6 and IL-8 (Jung et al., 2016). However, measurement of these is difficult and often dangerous due to invasive procedures (Jung et al., 2016). Less invasive options are measuring cytokines in the cervicovaginal fluid in order to help predict a woman's chance for PTL (Jung et al., 2016). Knowing that the cytokines are present contributes to the doctor's decision on how to treat the patient, but this alone is not enough to truly predict PTL (Jung et al., 2016). A combination of recognizing different

risk factors will help to lead to a better prediction on PTL and influence treatment decisions.

An important risk factor as an indication of PTL is cervical length in combination with fibronectin tests (van Baaren et al., 2014). Cervical length is tested to see if the cervix is a normal size or shorter than normal, as seen in Figure 2. A shorter cervix is an indicator of PTL (van Baaren et al., 2014). Fibronectin tests are done to see whether the cervix tests positively or negatively for fibronectin, where a positive test is an indicator of PTL (van Baaren et al., 2014). Alone, these tests will cause woman to be over treated and increase rates of trips to the hospital because it is difficult to determine low verse high-risk patients. However, together, the tests have good predictive capabilities for PTL. Woman can be considered low-risk for PTL with cervix lengths 30 mm or greater and lengths between 15 and 30 mm with negative fibronectin tests (van Baaren et al., 2014). Relatedly, woman can be considered high-risk for PTL with cervix lengths 15 mm or lower and lengths between 15 and 30 mm with positive fibronectin tests (van Baaren et al., 2014). Following these tests, doctors will know which patients to pay greater attention to in order to minimize the potential for PTL.

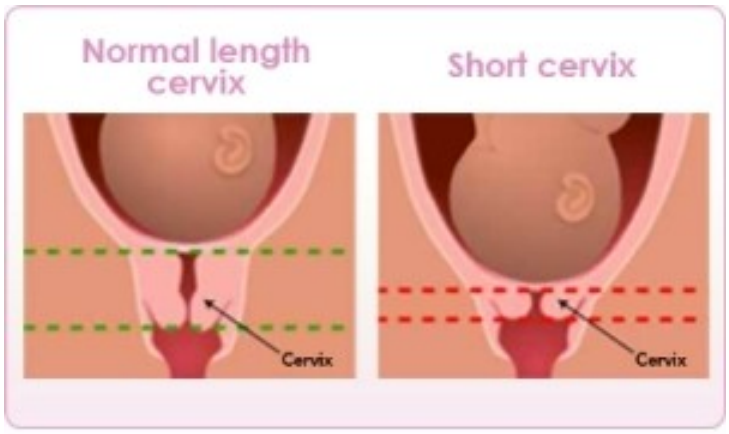


**Figure 2: Difference in cervical length. The first image seen is the normal cervical size, while the second image is a short cervix. Having a short cervix is a large indicator that someone will enter PTL. ("Short_cerix.jpg (301×225)," n.d.)**

Finally, an important part of the cervix is the CMP, as seen in Figure 3. The CMP is a viscoelastic material that acts as a block to bacteria from entering the cervix (Becher, Adams Waldorf, Hein, & Uldbjerg, 2009). When the cervical mucus is under the influence of progesterone, its properties become thick, viscous, and sticky, eventually forming the CMP that obstructs the cervical canal (Hein, Helmig, Schønheyder, Ganz, & Uldbjerg, 2001). The CMP could lose its ability to act as a block to bacteria when the ECM remodels incorrectly due to no longer being intact or adhering as tightly to the cervix (Becher et al., 2009). Normally, the CMP is shed when the cervix is between 4-10 cm of dilation, but during PTL it is shed earlier (Bastholm, Becher, Stubbe, Chronakis, & Uldbjerg, 2014). This early shedding of the CMP could indicate cervical incompetence and it is important to pay attention to the CMP's conditions (Becher et al., 2009). As a result of the crucial role the CMP plays in preventing PTL, a clinical way to use it as a

biomarker for pre-term labor is attempting to be established (Becher et al., 2009). Changes in cervical length or changes in surface tension, density, and viscosity of the plug could all be potential biomarkers but the relative importance of these factors on maintaining cervical competence is not known. The rheology and permeability of the cervical mucus for a low and high risk patient has been observed, but the specific properties of the CMP that are looked at in this experiment have not been studied (Critchfield et al., 2013). Rheology relates to the viscosity, but no values were stated; only that high-risk patients have a more viscous plug than low risk patients (Critchfield et al., 2013). All other properties of the CMP were not measured and their roles are unknown.


**Figure 3: Cervical mucus plug. This is an image of the plug outside of the body. It has viscoelastic properties, with both solid and liquid characteristics. (Becher et al., 2009)**

The purpose of this undergraduate research project is to develop a sophisticated computational model that simulates cervical remodeling during PTL and to use this model to investigate how changes in cervical biophysical properties influence PTL. The first goal is to test the mechanical properties of the cervical tissue to determine the

significance of them. Previous studies have looked at the mechanical properties of the female reproductive system, but they did not show the relation between the properties. Additionally, the Young's Modulus was the only factor measured for the system and other factors may have an important role in PTL (Baah-Dwomoh, McGuire, Tan, & De Vita, 2016). The main properties that will be looked at are Young's Modulus, force, and Poisson's Ratio. Studies of the mechanical properties are relatively rare compared to studies of cervical biochemical properties (House, Kaplan, & Socrate, 2009). The next goal is to test the mechanical properties of the CMP and see what effects they will have on the system. Surface tension, viscosity, and density will be the properties focused on for the CMP. Similarly, the research is trying to find the role that the CMP has in PTL in general and to rank its importance in relation to the cervical tissue. The CMP has not been modeled with the cervix before, which makes this portion of the project unique. The last goal was to test cervical length and see how this influences cervical length.

In total, four hypotheses were made for the model. The first one is that alterations in the cervical tissue biophysical properties will change the opening of the cervix. The second is that alterations in the CMP biophysical properties will change the opening of the cervix. The third is that the CMP acts as an important structure in regulating cervical opening. This is an overall statement that the CMP, with all of its properties combined, will be important in preventing PTL. Additionally, this is the most imperative hypothesis that was to be tested when conducting the experiment. The last hypothesis was to see if the model will support that cervical length has a large influence on cervical opening. If this is verified, it helps to show that the model is operating accurately.

CHAPTER 2: MATERIALS AND METHODS

## 2.1: General methods and schematics

In order to study the mechanical effects of PTL, the cervix and CMP are being modeled computationally using the COMSOL 5.2 finite element package. Currently, there have only been models of the cervix itself and studies of the CMP outside of the body. In this project, the cervix and CMP will be modeled together to see the effect one has on the other when PTL is triggered. This is a very difficult concept to model because the specific surface-fluid interactions used have not been incorporated into a model before. The main principles that are being looked at are how changes in the cervical tissue and CMP properties influence the degree of cervical opening.

Figure 4 shows the anatomical view of the cervix, which the models attempted to replicate. Looking at the cervix viewed from below, the CMP would sit in the hole between the walls. Figure 5 shows a schematic of the cervix. In this schematic, the blue structures signify the surrounding tissue that makes up the cervix. The red line at the top denotes the interface between the womb and the CMP, while the bottom blue line represents the interface between the vagina and the CMP. Finally, the yellow lines indicate the CMP. The model is a simplified depiction of the anatomical structures.

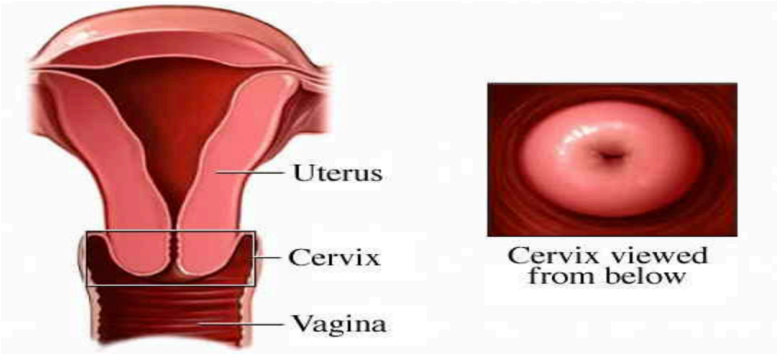

**Figure 4: General anatomical picture of the cervix. The first image shows an overview of the cervix, womb, and vagina. The second image shows what the cervix looks like when observed from below. (RN, n.d.)**

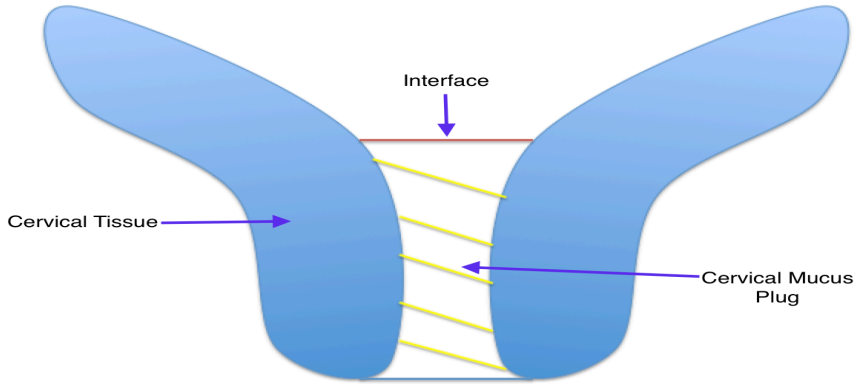


**Figure 5: Schematic of the cervix. This is a representation of what will be modeled when testing the biophysical properties. The main areas focused on will be the cervical tissue and the CMP and their interactions.**

## 2.2: Axial Symmetric Cylindrical Computational Model

The model created was a cylindrical computational model of the cervix and CMP, as seen in Figure 6. The type of system used was an axial symmetric one. Additionally, in an axial symmetric system, cylindrical coordinates are used. The traditional x-axis is called the r-axis, which is the radial direction; the traditional y-axis is called the z-axis, which is the axial direction; and the Phi axis is added, which is the circumferential direction. An axial symmetric system allows the user to build a 2-dimensional model that touches the line of symmetry. The part of the model that touches the line of symmetry will be revolved around it when the computation is run. Axial symmetry is governed by Equation 1, which means that the object cannot move in the r direction. This revolved

figure will represent the cervix and the CMP as a 3-dimensional object. The revolved model can be seen in Figure 7.

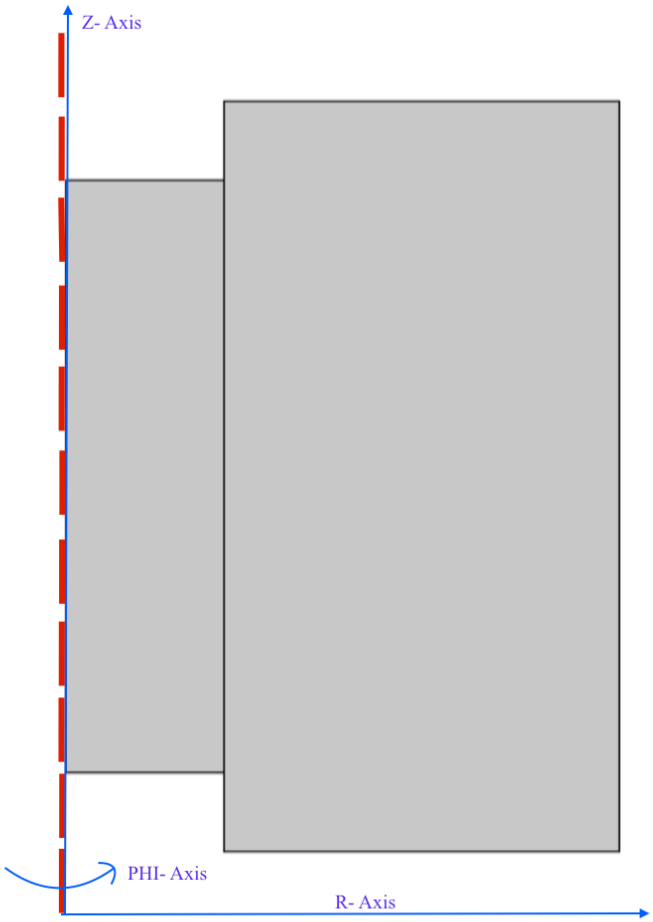


**Figure 6: Axial symmetric cylindrical computational model. The R-axis is the horizontal axis, the Z-axis is the vertical axis, and the PHI-axis is the axis that the model rotates around.**

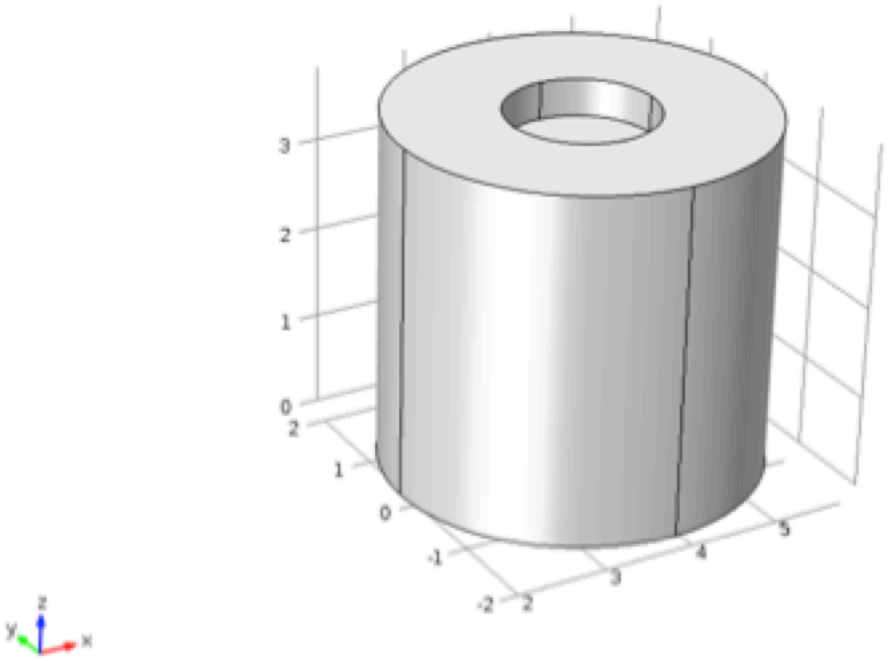


**Figure 7: 3-Dimensional revolution of the axial symmetric model. This is what the model looks like when the axial symmetric conditions are incorporated. The conditions act on all the boundaries uniformly to get the results.**

$$\frac{d}{dr} = 0 \tag{1}$$

To continue, the physics in the model were solid mechanics; laminar two-phase flow, moving mesh; and moving mesh. The solid mechanics physics was used to control the properties of the cervical tissue. The laminar two-phase flow, moving mesh was used to control the properties of the CMP, which is governed by Equations 2 and 3. Equation 2 is the Navier Stokes Equation, which is a conservation of momentum balance for fluids. Finally, the moving mesh was created to allow the model to remesh as each result was computed. Once the physic types were determined, the study chosen was time dependent.

Time dependent was used in order to see the progression of the modeling running during a certain time frame.

$$\rho\frac{d(\bar{u})}{dt} + \rho(\bar{u}2 * \nabla)\bar{u}2 = \nabla * [-\rho l + \mu(\nabla\bar{u}2 + (\nabla\bar{u}2)^T)] + \bar{F} \quad (2)$$

$$\rho\nabla * \bar{u}2 = 0 \quad (3)$$

A parameter section was created under global definitions. This was done in order to establish the baseline values of each property used within the model. For the CMP, the properties looked at were viscosity, density, and surface tension. Meanwhile, the properties focused on for the cervix were Young's Modulus, Poisson's Ratio, and force. Looking at Table 1 below, the baseline values for each parameter can be seen for the CMP. The actual mechanical property values of the CMP are not well known, but educated guesses were made to determine what should be used. The surrounding cervicovaginal mucus can be collected and the rheology observed, but it may not have the same properties as the CMP (Lai, Wang, Wirtz, & Hanes, 2009). Likewise, Table 2 shows the baseline values for the cervical tissue. The values of the Young's Modulus and Poisson's Ratio were known, while an educated guess was made for the force.

**Table 1: CMP Baseline Values**

| CMP | |
|---|---|
| Parameter (Units) | Value |
| Viscosity (Pa*s) | 1 |
| Density (Kg/m^3) | 1000 |
| Surface Tension (N/m) | 6.0E-2 |

**Table 2: Cervical Tissue Baseline Values**

| Cervical Tissue |
|---|

| Parameter (Units) | Value |
|---|---|
| Young's Modulus (kPa) | 1 (Kristin M. Myers, Hendon, et al., 2015) |
| Poisson's Ratio (unit less) | 0.3 (Kristin M. Myers, Hendon, et al., 2015) |
| Force (N) | 1 |

Two rectangles were built in the geometry section to create the model. The first, smaller rectangle, which represents the CMP, has the dimensions 0.8 cm wide and 3 cm long, starting 0.4 cm along the z-axis. It is touching the axial symmetric line, the red line in Figure 3, and the model was rotated around this when computed. The second, larger rectangle, which represents the cervical tissue, has the dimensions 2 cm wide and 3.8 cm long, starting at 0.8 cm along the r-axis (Kristin M. Myers, Hendon, et al., 2015). The CMP rectangle is smaller than the cervical tissue rectangle to represent that it spans the distance of the cervix, but does not fill the entire space.

The physics of the system were then added to the model when the geometry was finished. Figure 8 represents the large rectangle, which was given solid mechanics physics with multiple boundary conditions. It was run in quasi-static conditions so that inertia terms were ignored and it was considered a linear elastic material. The values for the linear elastic materials were defined in the parameter section of the model, as stated above. Equations 4 through 6 control linear elastic materials, which set the properties of the model to act elastically as forces are applied. Equation 5 represents the standard equation for stress and strain, while Equation 6 represents what "D" is equal to when under isotropic conditions. The model was initially run using isotropic conditions.

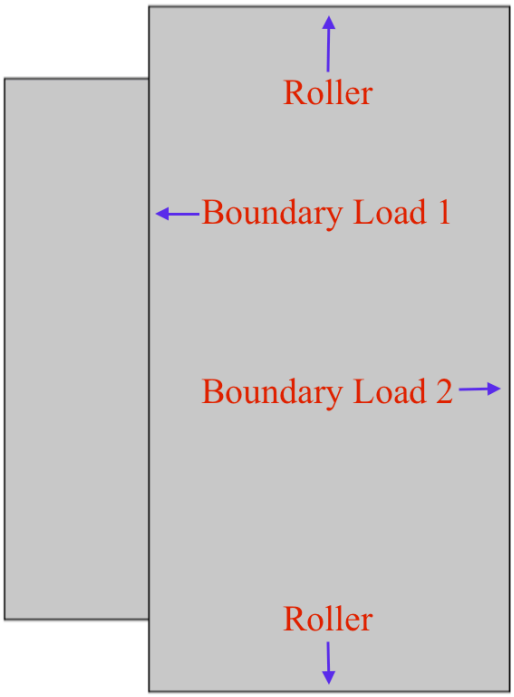


**Figure 8: Cervical tissue boundary conditions. These govern how the cervical tissue will operate when the model is run.**

$$\varepsilon = \frac{1}{2}[(\nabla \bar{w})^T + \nabla \bar{w}] \tag{4}$$

$$\begin{bmatrix} \sigma_x \\ \sigma_y \\ \sigma_z \\ \sigma_{xy} \\ \sigma_{yz} \\ \sigma_{xz} \end{bmatrix} = D \begin{bmatrix} \varepsilon_x \\ \varepsilon_y \\ \varepsilon_z \\ 2\varepsilon_{xy} \\ 2\varepsilon_{yz} \\ 2\varepsilon_{xz} \end{bmatrix} \tag{5}$$

$$D = \frac{E}{(1+v)(1-2v)} \begin{bmatrix} 1-v & v & v & 0 & 0 & 0 \\ v & 1-v & v & 0 & 0 & 0 \\ v & v & 1-v & 0 & 0 & 0 \\ 0 & 0 & 0 & \frac{1-2v}{2} & 0 & 0 \\ 0 & 0 & 0 & 0 & \frac{1-2v}{2} & 0 \\ 0 & 0 & 0 & 0 & 0 & \frac{1-2v}{2} \end{bmatrix} \tag{6}$$

Roller boundary conditions were added to the top and bottom edges of the rectangle. Equation 7 describes the roller boundary. In general, roller boundaries will constrain the model from moving in the normal direction, but it is free to move in the tangential direction. For this model, the roller boundary allowed the model to move along the r-axis, but not along the z-axis. As a result of these rollers, cervical dilation was modeled while cervical effacement was not. The cervix could not shorten, so effacement could not be measured. These rollers are not completely accurate because the cervix would be able to cause movement of the surrounding tissue, but without them the model would not have enough constraints and would not be able to run.

$$\hat{n} * \overline{w} = 0 \tag{7}$$

Boundary load conditions were also added to the model, which are controlled by Equation 8. A boundary load, boundary load 1, was applied to the section of the cervical tissue rectangle that is in contact with the CMP rectangle. This allows a force to be applied that makes the boundary move as the fluid would. The load type was a force per unit area and user defined in N/m^2, where the r parameter is -tpfmm.T_stressr and the z parameter was –tpfmm.T_stressz. This force was applied to represent that the cervical tissue and CMP are attached before the plug is released and will move together in the human body. Then, a final boundary load, boundary load 2, was applied on the outer edge of the cervical tissue rectangle to apply a force that causes the whole model to move. The force applied was a total force in N, where the r parameter was F*t and the z parameter was zero. “F” represents the force and was defined in the parameter section of the model.

Similarly, “t” represents the time and is defined by the time dependent study. This force is simulating the growth of the uterus as it pulls on the cervix. However, it is not the most anatomically accurate representation of the force.

$$\bar{F}_A = \bar{\bar{\sigma}} * \hat{n} \tag{8}$$

The boundary conditions were then added to the CMP, as seen in Figure 9. The laminar two-phase flow, moving mesh was applied to the smaller rectangle. The top and bottom edges of the rectangle were given a prescribed mesh displacement (PMD) condition, PMD 1. Both the r and z displacement were unselected, allowing the edges to move freely. This simulates that there is nothing constraining the top and bottom portions of the CMP in the body. An axial symmetry condition was applied to the left edge of the rectangle, which touches the line of symmetry. As a result, the model will rotate around this line. The fluid properties of the CMP were defined from a material and the values were established in the parameter section of the model. A wall condition, wall 2, with slip velocity was added to the boundary shared by both rectangles in order to have the fluid move with the solid. This condition represents the attachment of the CMP to the cervical tissue and the fact that they move together until the CMP is shed. Equation 9 governs wall conditions with slip velocities, where $u_w$ is the velocity of the wall and u2 is the velocity of the fluid. The r parameter was u*t, representing the r-axis movement of the solid with time, and the z parameter was w*t, representing the z-axis movement of the solid with time.

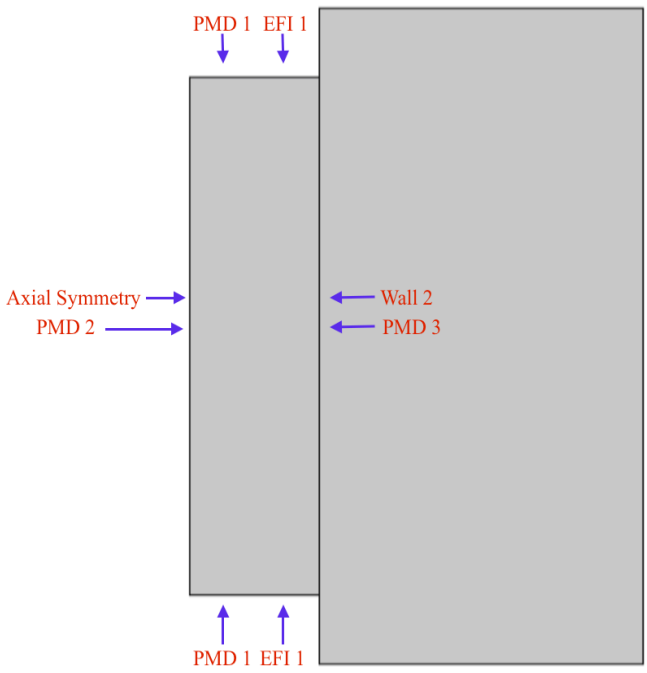


**Figure 9: CMP boundary conditions. These govern how the CMP will operate when the model is run.**

$$u_w = u2 \tag{9}$$

To continue, the top and bottom edge of the rectangle had an external fluid interface (EFI), EFI 1, with a user defined surface tension, ST, which was established in the parameter section. Equation 10 controls the EFI and it is an interface in which the viscosity in the fluid outside the domain can be neglected. $\bar{\sigma}_f$ represents the stress tensor, while $\gamma$ represents the surface tension and the overall equation is a balance of forces for the tissue and its surroundings. There is confidence in this equation because it used weak formulations to establish the boundary. This interface was created to represent that the

edges of the CMP interact with the surroundings. In real application, this condition signifies that the CMP has properties that keeps the overall material together until the surface tension is overcome by the load. Two more PMD conditions were added to model. PMD 2 was added to the left edge of the rectangle and defined as zero in the r displacement field in order to keep the edge of the fluid from moving along the r-axis. This condition is representing that the CMP will stay centrally located within the cervix as the cervix dilates, with the top and bottom edges of the CMP converging to the middle. PMD 3 was added to the right edge of the rectangle and in the z displacement, the value u*nr+w*nz was added. This condition was created to have the boundary move in the normal direction of the cervical tissue's r and z movement. This has the same application as wall 2 to represent that the CMP is attached and moves with the cervix.

$$n * \bar{\sigma}_f = p_{ext} * \hat{n} + \gamma(\nabla_t * \hat{n})\hat{n} - \nabla_t * \gamma \tag{10}$$

To finish creating the model, the moving mesh physics was added to both rectangles. The moving mesh physics is necessary because the model changes shape, and thus changes the needed mesh as the computation proceeds. Looking at Figure 10, a PDM condition, PDM 1, was applied to the left edge of the CMP rectangle. The r displacement was set at zero to keep the edge from moving along the r-axis. Then, both rectangle domains were applied with a free deformation condition with zero initial mesh displacement in both the r and z direction. For the cervical tissue rectangle, a PMD condition, PMD 2, was applied on all edges of the cervical tissue rectangle with the r displacement having the value of u and the z displacement having the value of w. This

allows the mesh to move as the solid does. Lastly, a PMD condition, PMD 3, was placed on the top and bottom edges of the CMP. No value was established in the r and z direction to allow the mesh of the plug in those areas to move freely. The mesh does not have an application in terms of real life, but it is necessary numerically to have the model run.

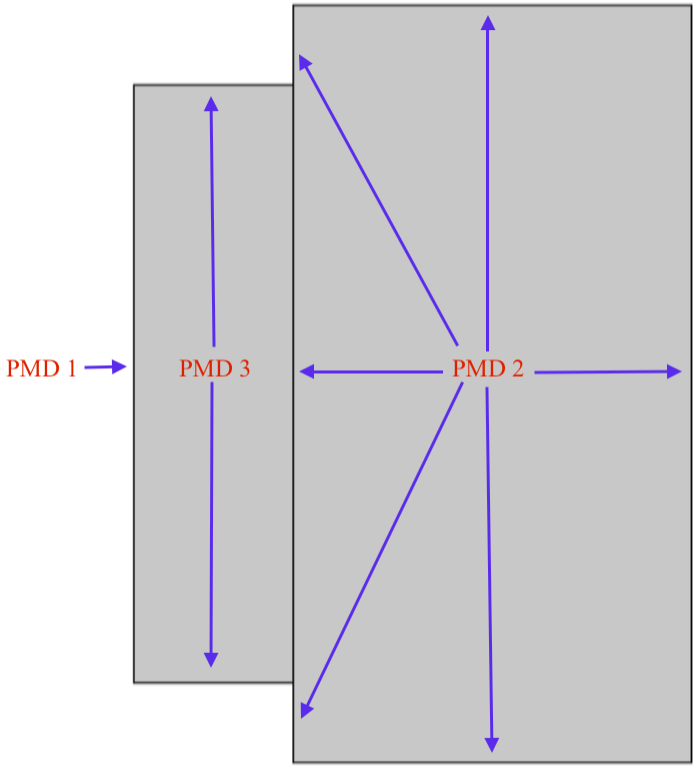


**Figure 10: Moving mesh boundary conditions. These govern how the moving mesh will operate when the model is run.**

The main boundary that posed difficulty in the model was the shared one between the fluid and the solid. For this boundary, fluid structure interactions had to be incorporated. Equations 11 through 13 governed the conditions controlling the boundary. First, Equation 11 represents the displacement of the structure, where the fluid displacement is equal to the solid displacement. Second, Equation 12 represents the stress of the fluid domain exerted as a boundary load on the solid. This is important to control how the two interfaces interact with each other. Finally, Equation 13 represents that the velocity at the wall is continuous. The left part of the equation is for the velocity of the fluid, while the right side of the equation is for the velocity of the solid. Limitations in the model occurred at this step since the CMP was unable to slip along the fluid structure boundary.

$$\overline{d}_f = \overline{d}_s \tag{11}$$

$$\overline{\overline{\sigma}}_f * \hat{n} = \overline{\overline{\sigma}}_s * \hat{n} \quad where\ \overline{\overline{\sigma}}_f = -\rho\delta + \mu(\nabla\overline{u} + \nabla^T\overline{u}) \tag{12}$$

$$\hat{n} * \overline{u} = \hat{n} * \frac{d\overline{w}}{dt} \tag{13}$$

In order to determine the type of mesh quality that should be run for the tests, a mesh plot study was conducted. The model was run with baseline conditions with varying mesh types to see where the results converge to get the most accurate data points. The types of mesh used were extra fine, finer, fine, normal, and coarse. These are incremental steps in mesh quality, where extra fine incorporates a large amount of degrees of freedom and coarse incorporates few degrees of freedom. Degrees of freedom represent the amount of meshing in the model.

After this model was created, the parameters were altered to see the effect of the plug and the cervix on PTL. The model was run with the baseline values initially and then each parameter was altered alone to see the effect that it would have on the model. The values were changed within a range of two orders of magnitude smaller than the baseline to two orders of magnitude larger than the baseline. A parametric sweep was used to run new values of one parameter while keeping the other parameters at the same value. Each of the CMP parameters was also varied with different Young's Modulus and force values to see the effect it would have on the system. Once a solution was determined, the distance the plug moved was computed using Equation 14. The distance was calculated by taking a point evaluation of the top left corner of the CMP rectangle. After this value was found, it was subtracted from the total size of the plug, 3.4 cm, and multiplied by two in order to establish the size change. The distance traveled was multiplied by two due to the fact that the plug was moving in from both the top and bottom and the point evaluation only calculated the movement of the plug from the top. Finally, using Equation 15, the percentage opening of the cervix was determined to see how each factor affected the system.

$$Plug\ size\ change = (3.4 - Distance\ top\ left\ point\ moved) * 2 \quad (14)$$

$$Percentage\ Opening = \frac{Plug\ size\ change}{Initial\ plug\ size} * 100 \quad (15)$$

Each computation of the model was run under isotropic conditions, as stated above, with a time dependent study. For the time dependence, it started at time point zero and took a 0.1 second time step until reaching 1 second. This was used since the cervix

has a nonlinear, time-dependent stress response (K. M. Myers, Paskaleva, House, & Socrate, 2008). Additionally, automatic remeshing was added in order for the model to alter its mesh as the computation changed the geometry. For the automatic remeshing, it was set to remesh at the last step taken by the solver before it stopped. The variance for the parameters was in a range within two orders of magnitude, in both positive and negative directions, to get a large number of data points. This was done because the true important range of the parameters is unknown. After all the percentage openings were calculated, plots were created to show the affect each factor had on the system.

Once the model was completed and all factors computed in isotropic conditions, the next step taken was to run Figure 6 with orthotropic, quasi-static conditions. This was done because it would be a more accurate representation of the tissue within the body. The collagen fibers within the cervix preferentially align in different directions (Kristin M. Myers, Socrate, Paskaleva, & House, 2010). The standard equation for stress and stress, Equation 5, and Equations 16 through 26 governs the orthotropic conditions of the model. All the parameters were kept the same except for Young's Modulus, which was altered in the R, Phi, and Z directions. Figure 11 represents these orientations, with R, PHI, and Z as the red, green, and blue lines respectively. Changes in R represented the radial direction, changes in Phi signified the circumferential direction, and changes in Z denoted the axial direction. When the Young's Modulus was adjusted in the R direction, it would be multiplied by a factor ranging between one and ten, while the other two directions were kept at a constant Young's Modulus. The same was done for the other two factors. To continue, The Poisson's Ratio was kept constant in all three directions,

with a value of 0.3. Similarly, the shear modulus was kept constant in all three directions using Equation 27.

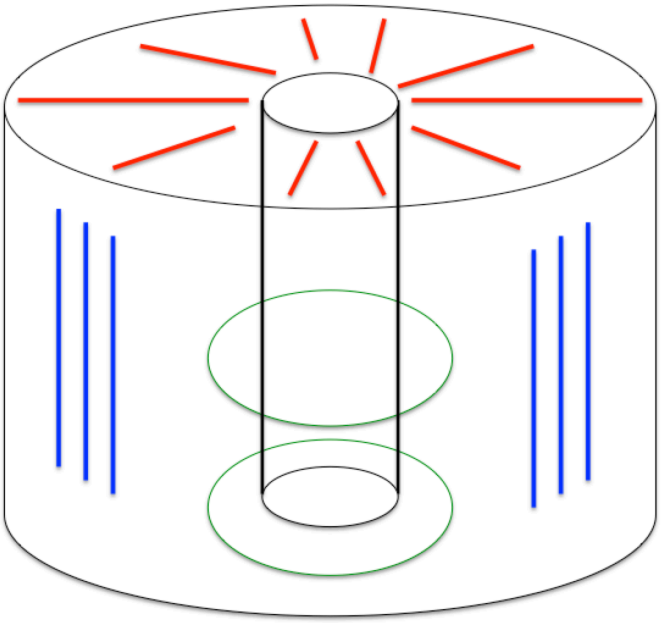

**Figure 11: Fiber alignment of the cervical tissue in the orthotropic direction. These govern how the directional conditions will operate when the model is run.**

$$D = \begin{bmatrix} D_{11} & D_{12} & D_{13} & 0 & 0 & 0 \\ D_{12} & D_{22} & D_{23} & 0 & 0 & 0 \\ D_{13} & D_{23} & D_{33} & 0 & 0 & 0 \\ 0 & 0 & 0 & D_{44} & 0 & 0 \\ 0 & 0 & 0 & 0 & D_{55} & 0 \\ 0 & 0 & 0 & 0 & 0 & D_{66} \end{bmatrix} \tag{16}$$

$$D_{11} = \frac{E_x^2(E_z v_{yz}^2 - E_y)}{D_{denom}} \tag{17}$$

$$D_{12} = -\frac{E_x E_y(E_z v_{yz} v_{xz} + E_y v_{xy})}{D_{denom}} \tag{18}$$

$$D_{13} = -\frac{E_x E_y E_y(v_{xy} v_{yz} + v_{xz})}{D_{denom}} \tag{19}$$

$$D_{22} = \frac{E_y^2(E_z v_{xz}^2 - E_x)}{D_{denom}} \tag{20}$$

$$D_{23} = -\frac{E_y E_z\left(E_y v_{xy} v_{xz} + E_x v_{yz}\right)}{D_{denom}} \tag{21}$$

$$D_{33} = \frac{E_y E_z\left(E_y \mathrm{v}_{\mathrm{xy}}^2 - E_x\right)}{D_{denom}} \tag{22}$$

$$D_{44} = G_{xy} \tag{23}$$

$$D_{55} = G_{yz} \tag{24}$$

$$D_{66} = G_{xz} \tag{25}$$

$$D_{denom} = E_y E_z v_{xz}^2 - E_x E_y + 2 v_{xy} v_{yz} v_{xz} E_y E_z + E_x E_z v_{yz}^2 + E_y^2 v_{xy}^2 \tag{26}$$

$$G = \frac{E}{2*(1+\nu)} \tag{27}$$

This was also run as time dependent, but the range of time was varied compared to the isotropic conditions. For the time dependence, it started at time point zero and took a 0.05 second time step until reaching 0.9 seconds. Similarly, for the automatic remeshing, it was set to remesh at the last output from the solver before it stopped. The conditions were altered because the model was having convergence issues when using the isotropic time dependent settings. Again, the percentage opening for the cervix was calculated for each parameter using Equation 15. The results of the computations were then plotted together to see which direction affected cervical opening the most.

Another test run was calculating the cervical length. In order to incorporate the multiple sizes that the cervical tissue can be, it was varied from 14 mm to 38 mm. The cervical tissue and CMP were scaled proportionally to each other to run at smaller sizes. Equation 28 was used to calculate the new CMP length based on the cervical tissue. Once the new sizes were determined, the model was run with baseline values under the

isotropic conditions used before. The results were then plotted to see the effect that cervical size has on the percent opening. Certain CMP parameters were also altered at a cervix length of 17 mm to test the important of the CMP with a short cervix. The idea was to see if the CMP's role changed with different sized cervixes.

$$New\ CMP\ size = \frac{New\ cervical\ tissue\ size}{Original\ cervical\ tissue\ size} * Original\ CMP\ size \qquad (28)$$

Sensitivity analysis was also completed in order to determine which properties were more important than others. Equations 29-32 were used in order to calculate the sensitivity (Singh A.K & Bhadauria B.S, 2009). Equation 29 is the first order derivative for the initial value. Equation 30 is the first order derivative for the second through the second to last value. Equation 31 is the first order derivative of the last value recorded. Lastly, Equation 32 uses the previous three equations to calculate sensitivity.

$$f'(x_o) = -\frac{(2h_1+h_2)}{h_1(h_1+h_2)}f_o + \frac{h_1+h_2}{h_1h_2}f_1 - \frac{h_1}{(h_1+h_2)h_2}f_2 \tag{29}$$

$$f'(x_1) = -\frac{h_2}{h_1(h_1+h_2)}f_o - \frac{h_1-h_2}{h_1h_2}f_1 + \frac{h_1}{(h_1+h_2)h_2}f_2 \tag{30}$$

$$f'(x_2) = \frac{h_2}{h_1(h_1+h_2)}f_o - \frac{h_1+h_2}{h_1h_2}f_1 + \frac{h_1+2h_2}{(h_1+h_2)h_2}f_2 \tag{31}$$

$$Sensitivity = \frac{Parameter\ value * f'(x_n)}{Percent\ opening\ at\ the\ parameter\ value} \tag{32}$$

CHAPTER 3: RESULTS AND DISCUSSION

The first step taken when determining results was running the mesh plot study. Looking at Figure 12, it can be seen that the mesh qualities all provided similar percent openings. As a result, the type of mesh used could be any since the convergence was so close. However, an extra fine mesh was chosen as an extra precaution in order for the model to run successfully. Some of the computations, with intricate remeshing, would not be able to run without a high mesh quality.

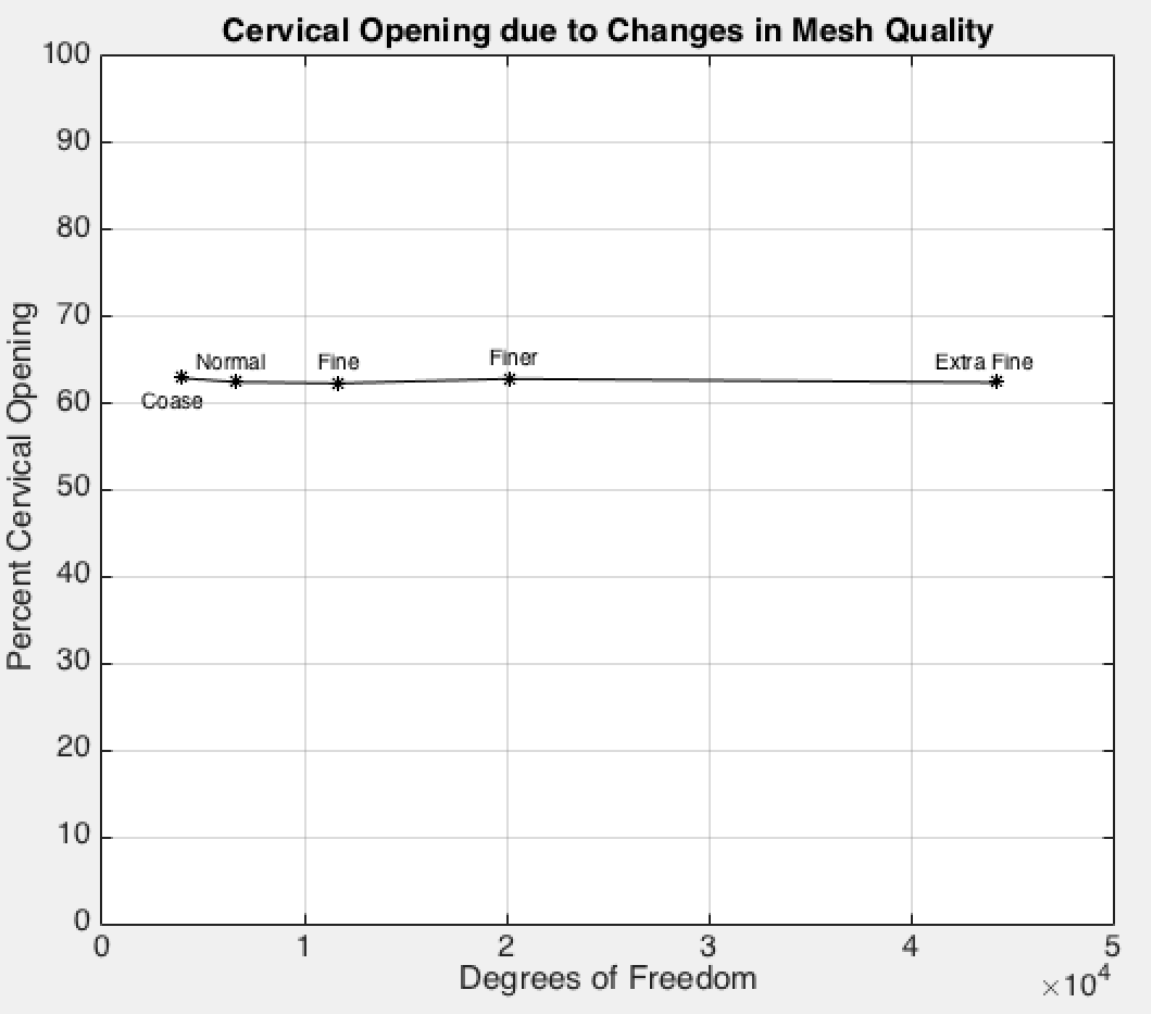


**Figure 12: Mesh independent plot study. This models the degrees of freedom against percent cervical opening to determine the best mesh quality to use.**

Multiple plots were created based off of the axial symmetric model to display the computational results. Based off these plots, the significance of each factor could be seen in relation to its ability to cause a change in cervical opening. Initially, the cervical tissue factors were computed. After the model was run, Figure 13 shows the 2-dimensional movement of the cervical tissue. It can be seen that the tissue moves out to a further position, with the highest stress on the boundary shared with the CMP. Similarly, Figure 14 shows the 3-dimensional movement of the cervical tissue. Again, it can be seen that the stresses are highest in the middle boundary and decrease as it reaches the edge of the tissue.

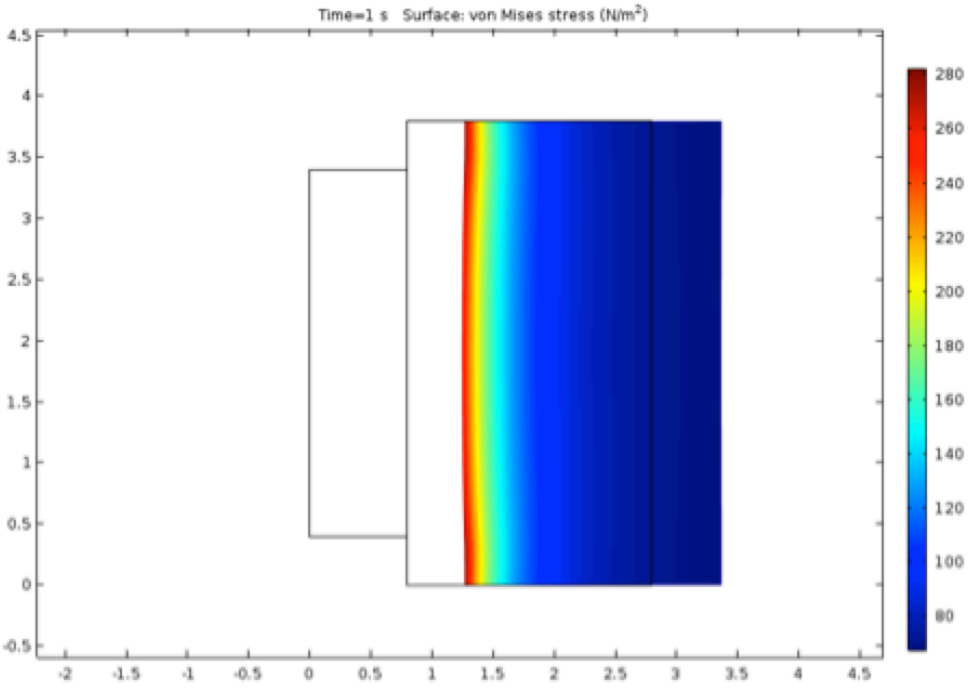


**Figure 13: 2-Dimensional view of von Mises stress on the cervical tissue. This shows the movement of the cervical tissue after the model was run.**

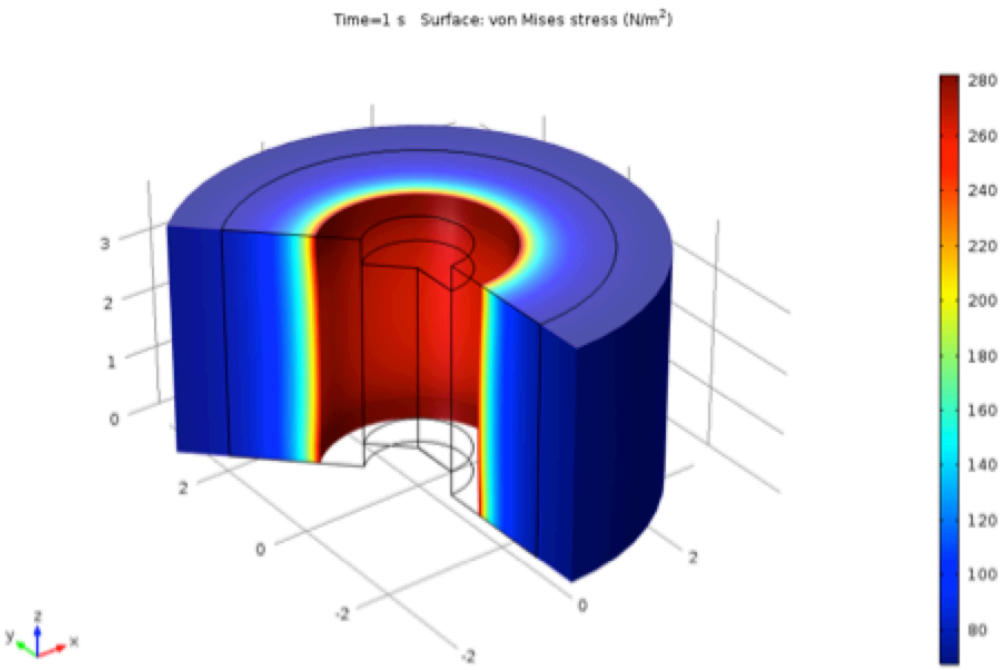


**Figure 14: 3-Dimensional view of von Mises stress on the cervical tissue. This shows the movement of the cervical tissue after the model was run when the revolution of the material occurred.**

The first factor tested was Poisson's Ratio and based off of Figure 15, it did not cause a meaningful change in cervical opening. The Poisson's Ratio created a greater opening with bigger values, yet it still was not a large value. From the data, it was concluded that the Poisson's Ratio does not have a great role in the causes of PTL. In terms of the body, a hypothesis as to why Poisson's Ratio does not play a role is that the change in deformation is not on a large scale for the cervix. As a result, the cervix is still able to dilate at a similar rate. The Poisson's Ratio probably does not reach the high values because at these points, it would be considered incompressible. If the material is

incompressible, then the cervix would not be able efface and dilate as it is supposed to and would not be able function correctly.

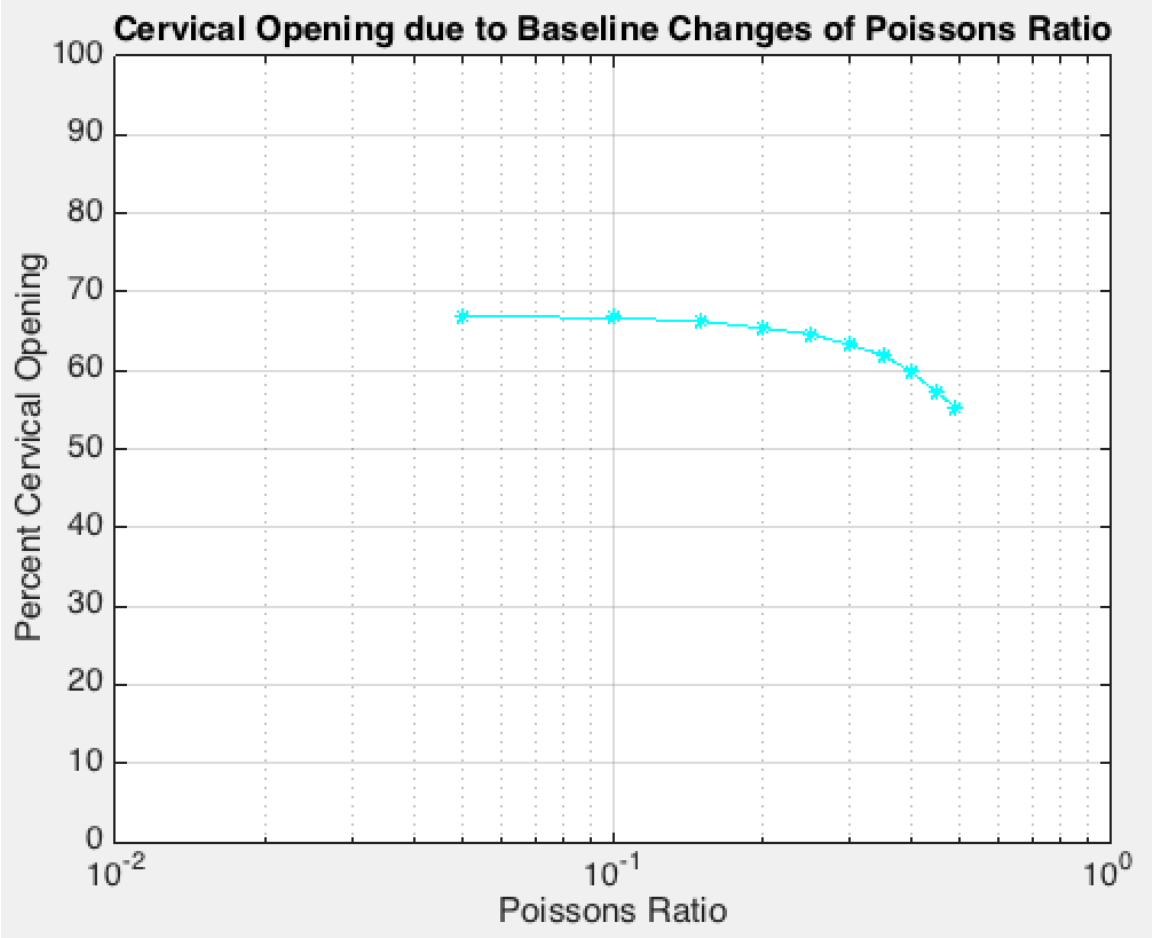


**Figure 15: Cervical opening due to baseline changes in cervical tissue Poisson's Ratio. This plots shows the effect Poisson's Ratio has on PTL.**

The next factor looked at for the cervical tissue was force. Looking at Figure 16, force does play a significant role in percentage cervical opening. Going through the range of values for force, it can be seen the percent cervical opening was just fewer than ten percent at the lowest force value and reach approximately 100 percent with the largest force value. Force was considered to play a big role in the mechanisms of PTL and it is

important to consider fit when monitoring cervical tissue since it could help to predict PTL and potentially save more lives.

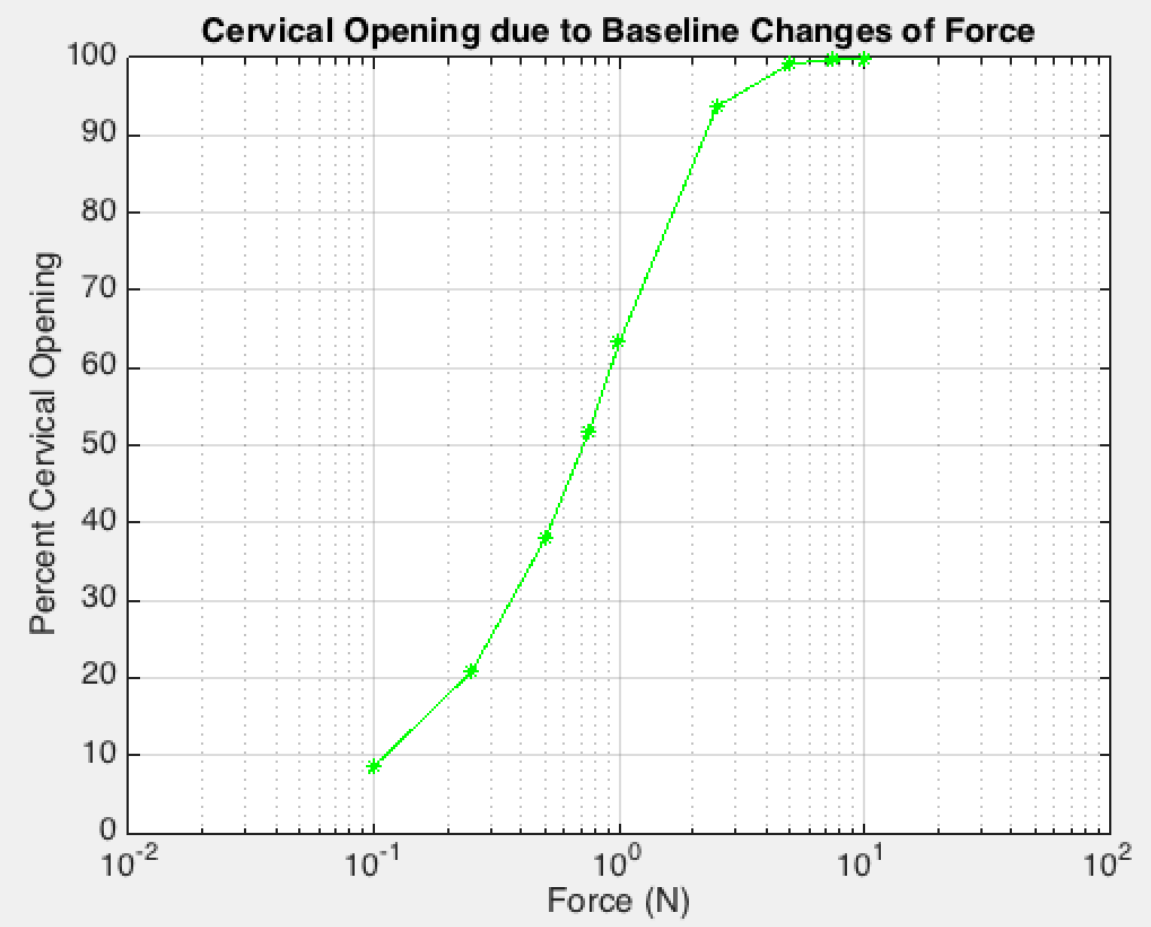


**Figure 16: Cervical opening due to baseline changes in cervical tissue force. This plots shows the effect force has on PTL.**

The last factor calculated for the cervical tissue was the Young's Modulus. From observing Figure 17, it can be seen that the Young's Modulus also had a noteworthy impact on the percentage cervical opening. It acted like the reciprocal of force, where the small values cause large percent openings and the large values caused small percent openings. This is because the tissue is stiffer and harder to pull apart at high values. As a

result, the Young's Modulus was also considered a major factor in leading to PTL and should be closely observed. Looking at the literature, 0.5 to 0.8 kPa represents the fits to the highest and lowest compression stress response reported for the tissue (Kristin M. Myers, Hendon, et al., 2015). However, another study stated that the ranges of the Young's Modulus were 2.17-243 kPa for the cervix (Baah-Dwomoh et al., 2016). From this, it is not clear what the main range that one should look at is so a large range needed to be computed to evaluate the importance of Young's Modulus.

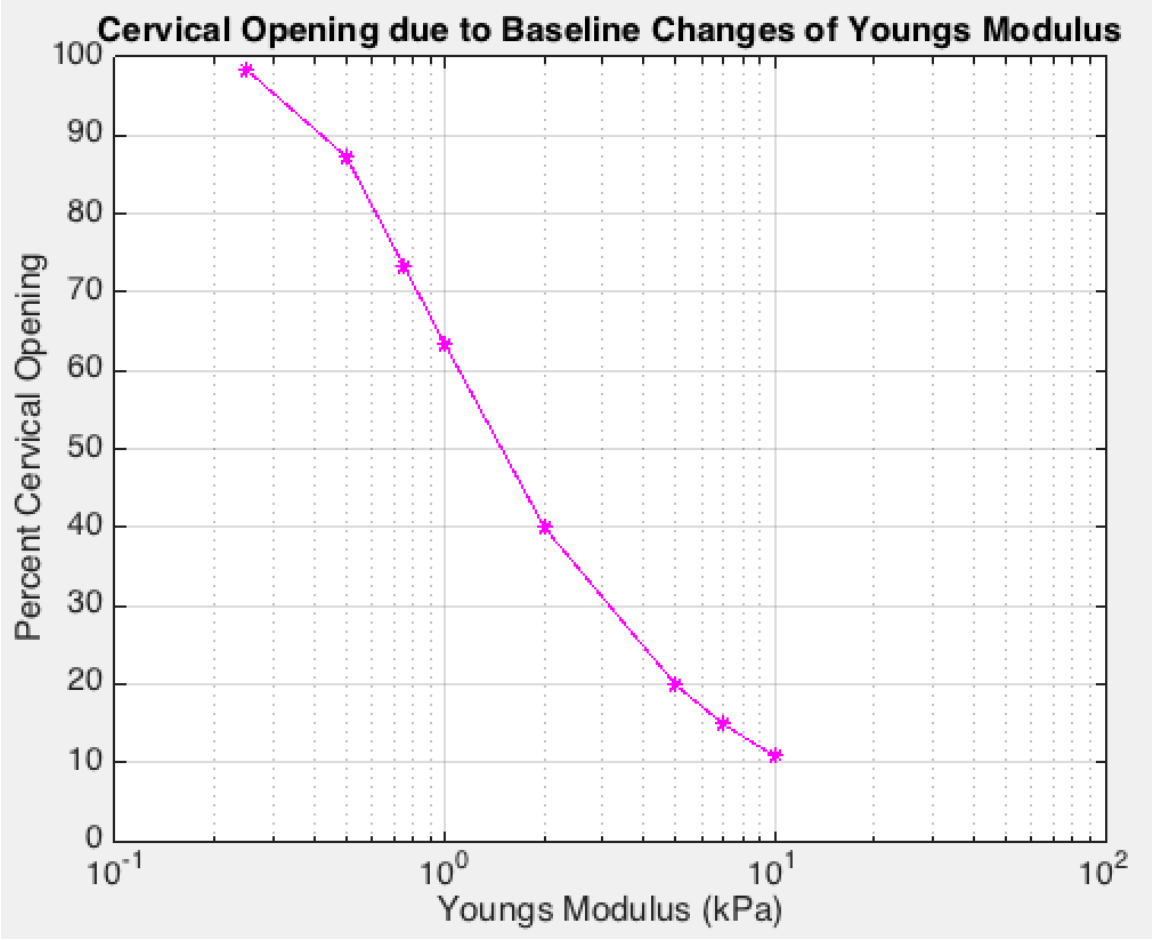


**Figure 17: Cervical opening due to baseline changes in cervical tissue Young's Modulus. This plots shows the effect Young's Modulus has on PTL.**

Once the cervical tissue factors were computed, the CMP factors were tested. Each of the properties was varied against different Young's Modulus and force values. The reason for this was to see how the mechanical properties of the plug changed as the important factors in the cervical tissue changed. Both Young's Modulus and force had significant roles in the cervical tissue, so they could potentially cause changes in how the CMP properties affected the system. Looking at Figures 18 and 19, the velocity of the plug can be seen in 2 and 3-dimensions. The stresses along the top and bottom edges of the CMP, where it curves in, are the highest, while the stresses at the center of the CMP are the lowest. This is due to the fact that the forces are expressed on the edges, rather than the center of the figure.

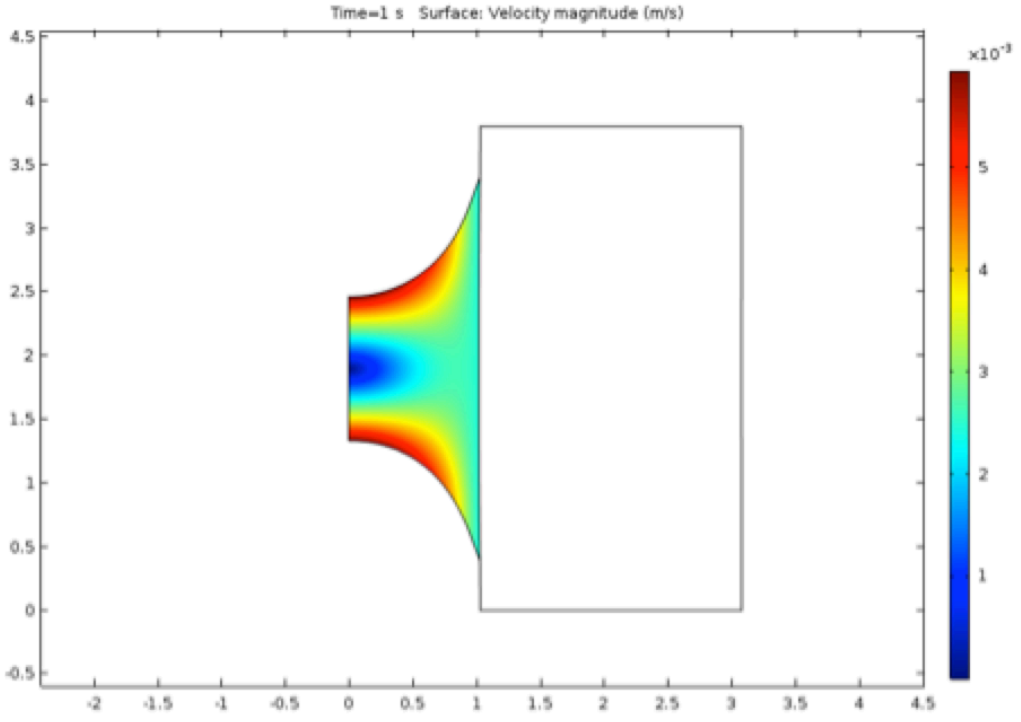


**Figure 18: 2-Dimensional view of the velocity of the CMP. This shows the movement of the fluid after the model was run.**

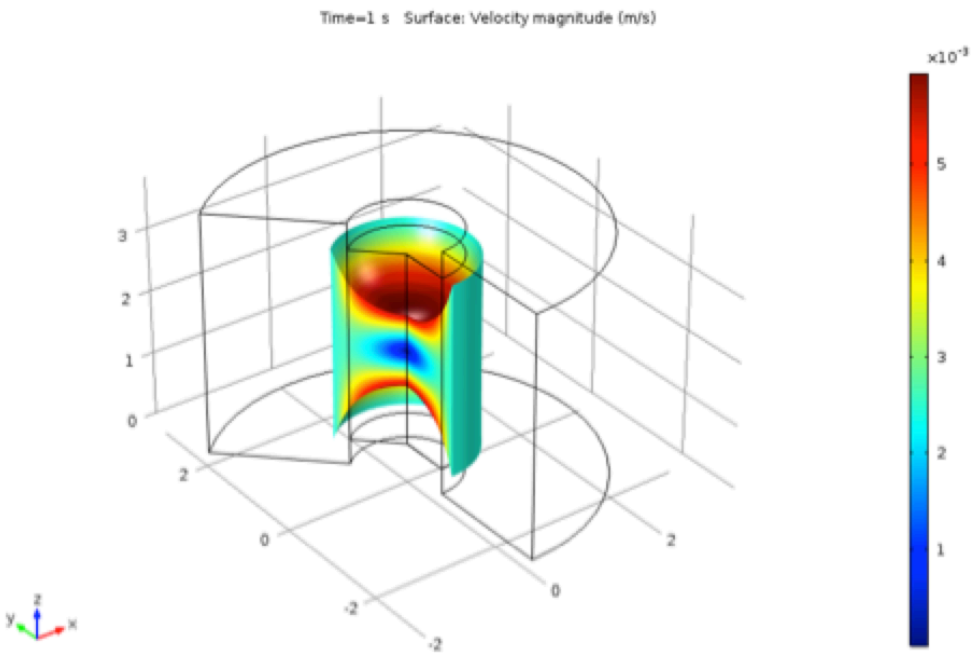


**Figure 19: 3-Dimensional view of the velocity of the CMP. This shows the movement of the CMP after the model was run when the revolution of the material occurred.**

The first factor measured was the viscosity of the CMP. Looking at Figures 20 and 21, altering the viscosity with varying Young's Modulus and force values did not have a large effect on cervical opening at small values. It started to have a larger effect as the viscosity became larger and this could potentially be important. As a result, the viscosity may be considered to play a role and it cannot be dismissed as entirely insignificant. An explanation of why viscosity may play a role is because it could reach the high values within the body. The CMP would then resist opening and be important in preventing PTL. However, the viscosity is most likely not going to reach the high values within the body. The main range for the viscosity when considering cervical mucus as a non-Newtonian was between $10^{-1}$ and $10^{0.5}$ Pa*s, which is in the horizontal region of the

viscosity graphs (Lai et al., 2009). But this range may not be as important for this model since the plug was modeled as a Newtonian fluid.

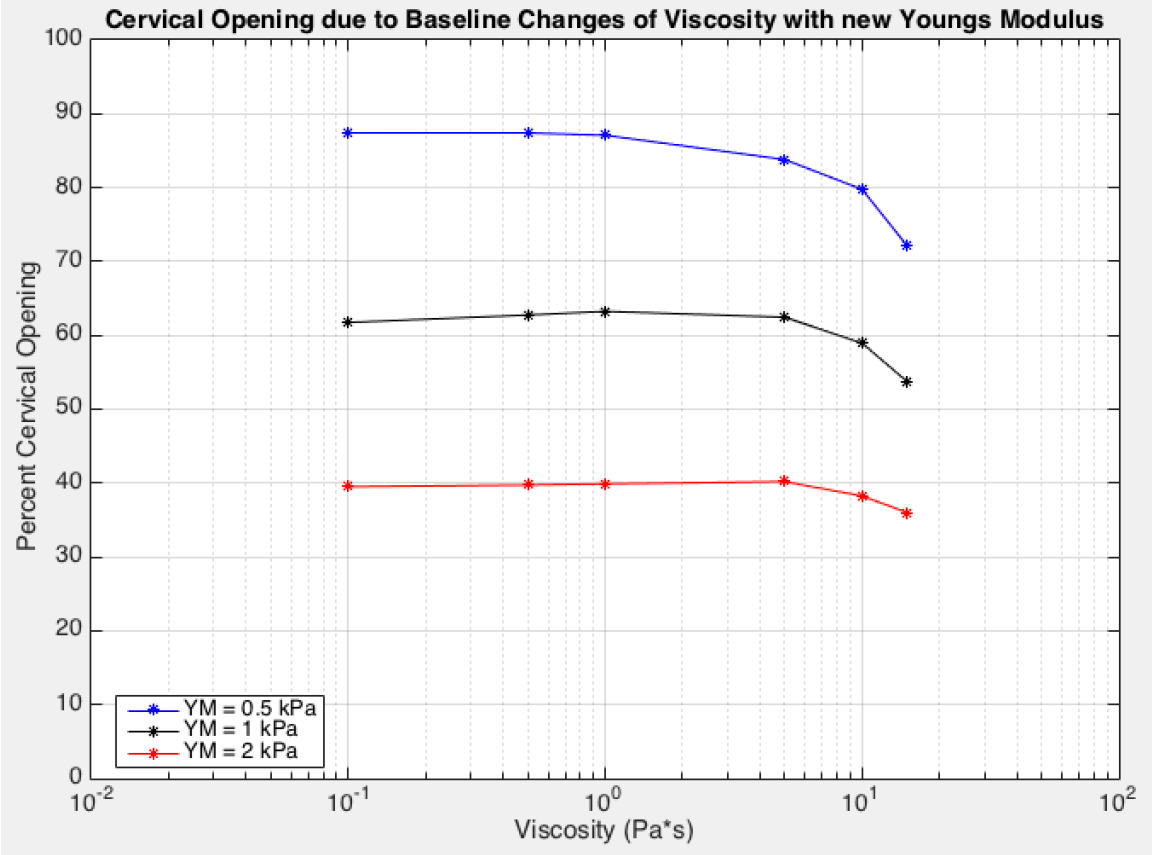


**Figure 20: Cervical opening due to baseline change in CMP viscosity with varying Young's Modulus values. This plots shows the effect viscosity has on PTL.**

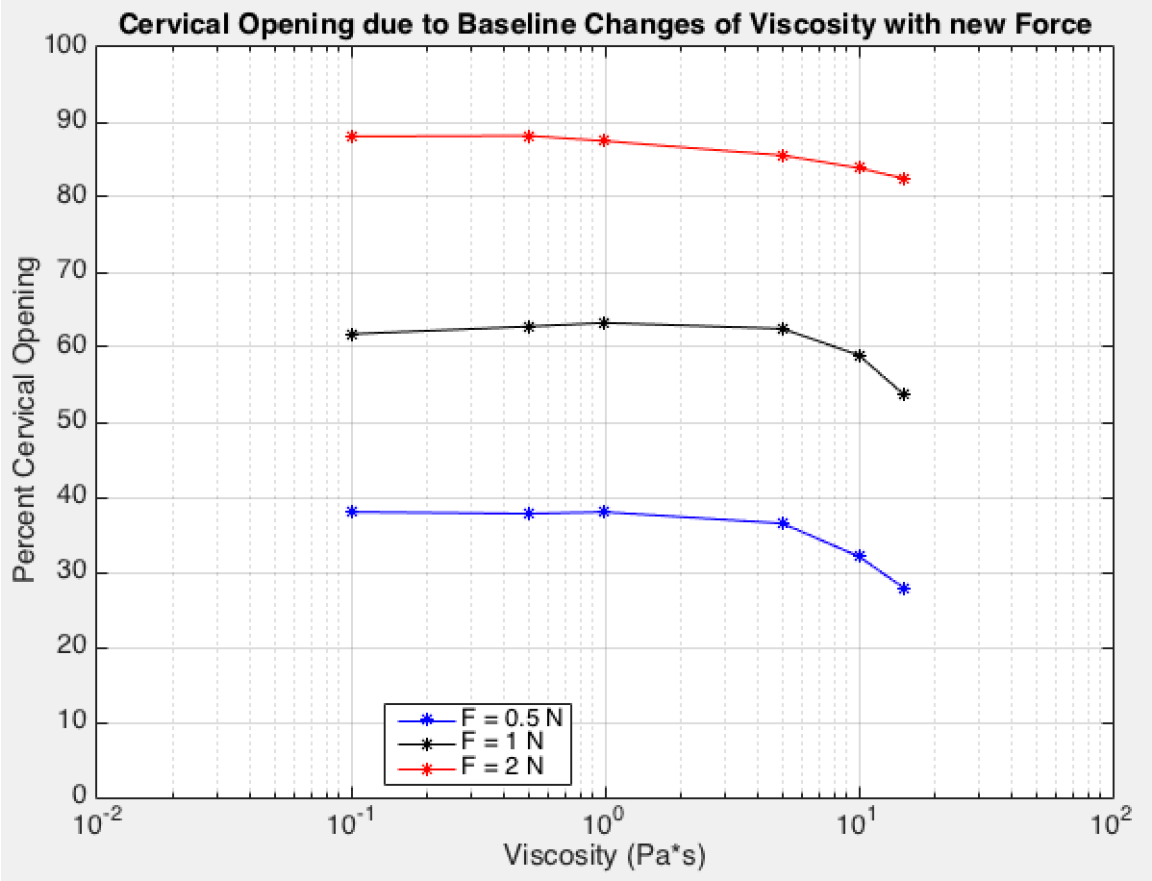


**Figure 21: Cervical opening due to baseline change in CMP viscosity with varying force values. This plots shows the effect viscosity has on PTL.**

The next factor considered was the surface tension of the CMP. Looking at Figure 22 and 23, the surface tension caused a slight change in cervical opening with varying Young's Modulus and force values. These were mainly when the values were larger than baseline, but they still were not substantial. The surface tension had a downward trend, where the higher values lead to lower percent openings, but not by very much. Due to the little change in cervical opening, surface tension was also not considered important in PTL.

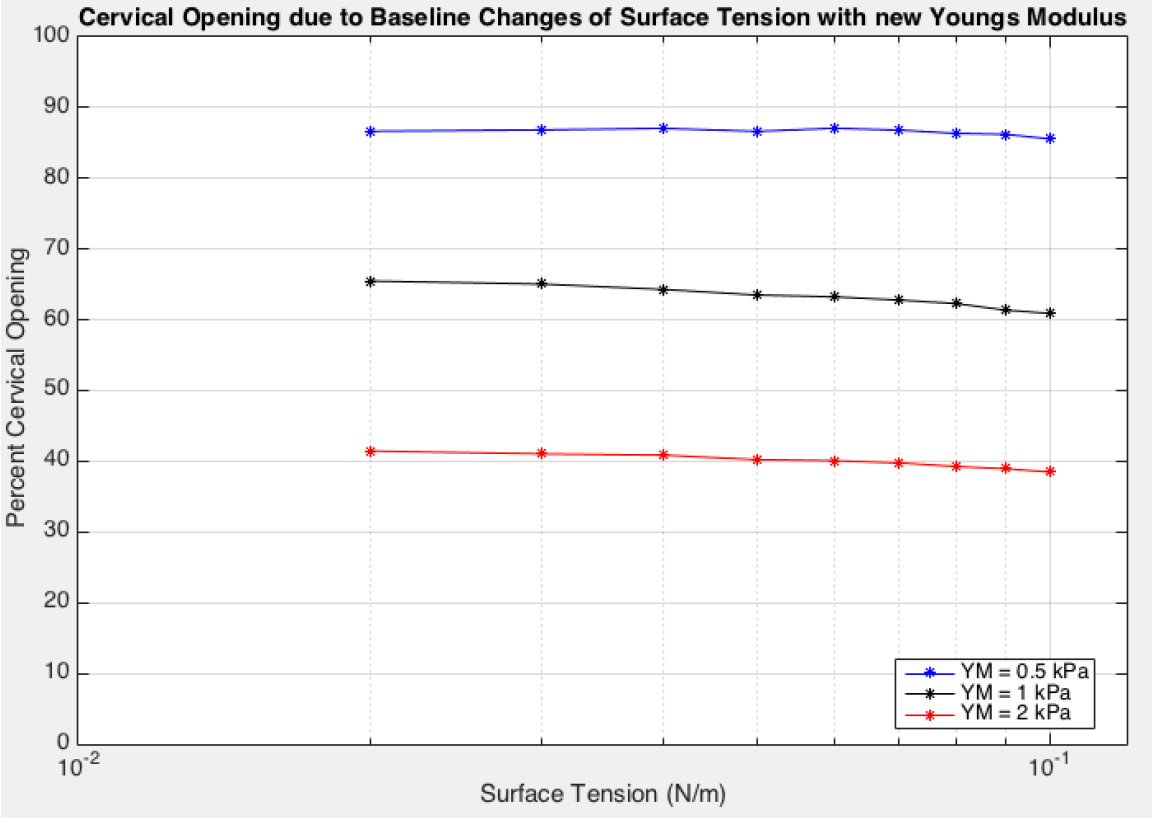


**Figure 22: Cervical opening due to baseline change in CMP surface tension with varying Young's Modulus values. This plots shows the effect surface tension has on PTL.**

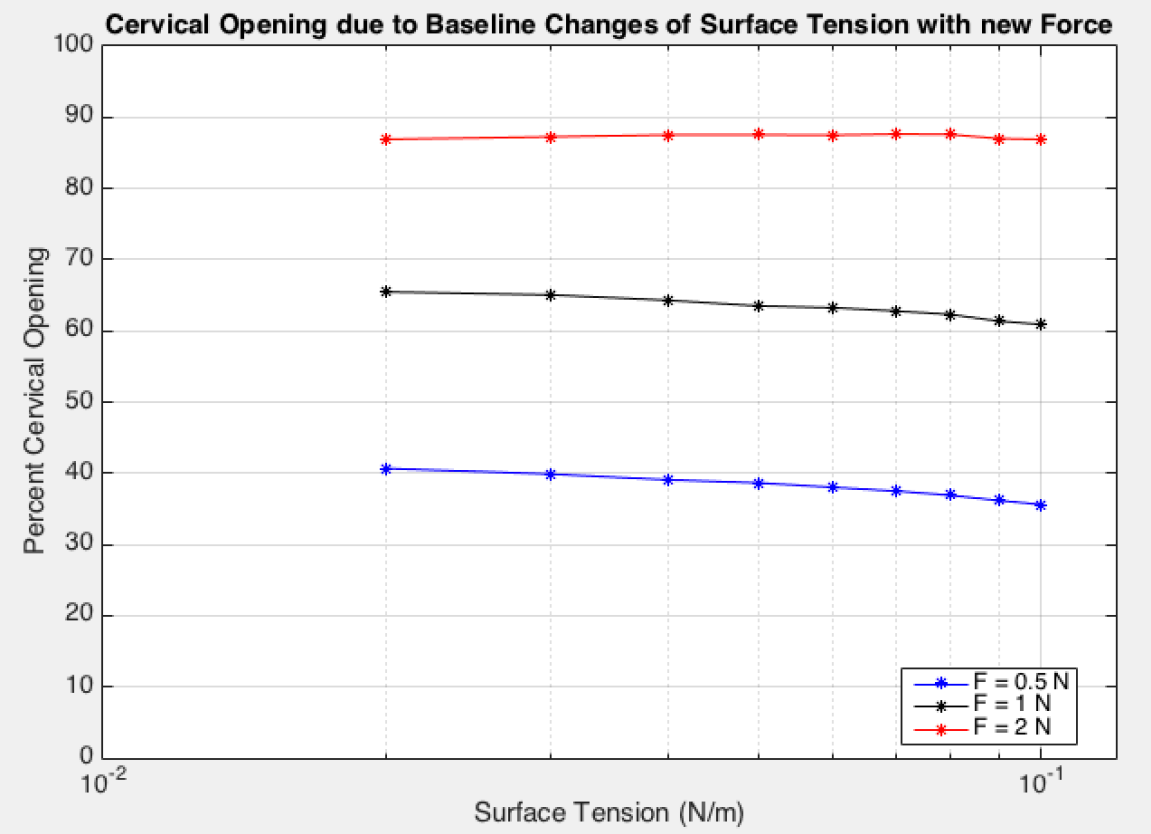


**Figure 23: Cervical opening due to baseline change in CMP surface tension with varying force values. This plots shows the effect surface tension has on PTL.**

The fact that surface tension does not play a big role in cervical opening is rather surprising since the high surface tension values should be very difficult to pull apart. Biologically, one guess as to why it does not play a large role is that the adhesion of the plug to the cervix is not very strong. As a result, the plug would fall out relatively early in the process and not affect the system. Another guess is that the plug is much smaller than the cervix, so the forces of the cervical tissue are even able to overcome very high surface tensions. However, the most likely guess as to why surface tension is not important is due to limitations of the model. The point contacts that the fluid and the surface have are

unable to slip along the shared boundary, as seen in Figure 24. If the points slipped, the two points would not be in the same place on the boundary and would rather have moved closer together. With the movement, the shape of the plug would look closer to an elongated rectangle, modeled in Figure 25. This means that the plug is not getting thinner as a unit, like it usually would if the point could slip, and the forces are not distributed as evenly on the CMP. If the points could slip, then it is believed that surface tension would potentially play a larger role in cervical opening.

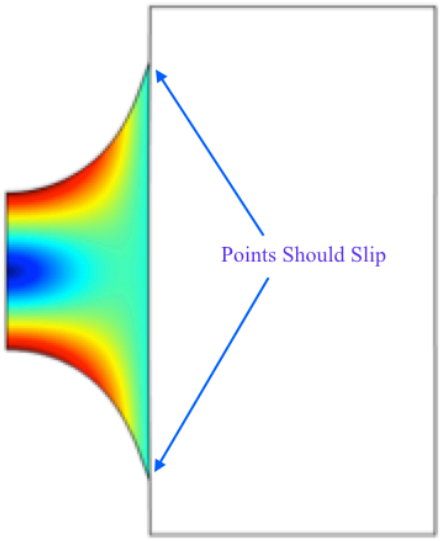


**Figure 24: Points that should slip in model. This could alter the effect that surface tension has on the system.**

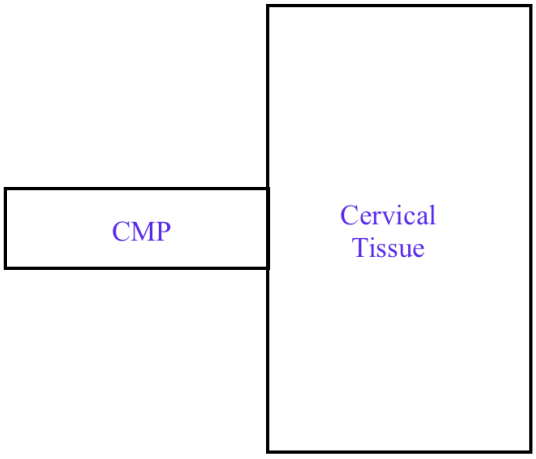


**Figure 25: Model if points slipped. The CMP would be more stretched and the top and bottom boundaries would have greater tension values.**

The final CMP factor looked at was density. Based off Figure 26 and 27, it can be seen that changes in density from the baseline value with varying Young's Modulus and force values did not cause striking changes in cervical opening. The trend seen looks as if a change in density has almost no effect on the percent cervical opening. Consequently, density was not considered as a central factor in cervical opening. Looking at the biological system, a reason that density does not play a role is that the volume of the plug does not change by a great amount. This would mean that the density does not vary largely as the plug is pulled part, leading to little effect on cervical opening.

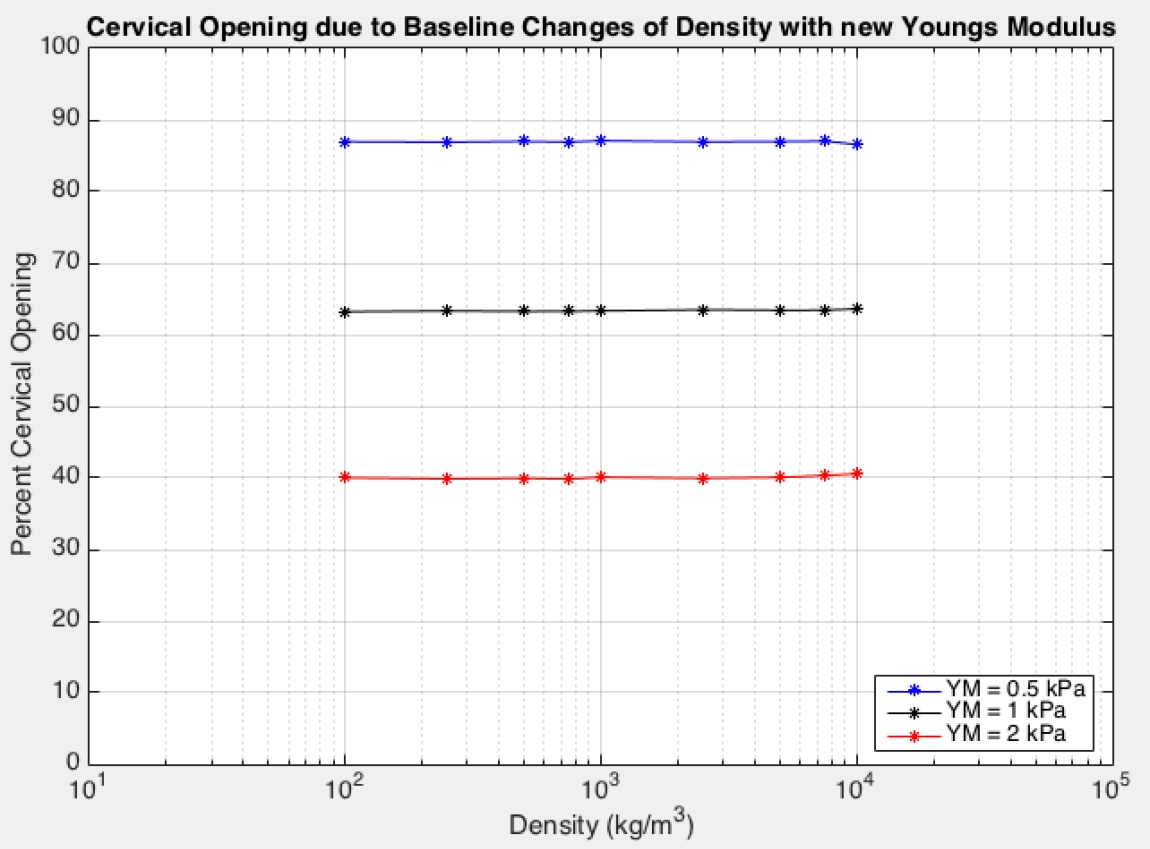


**Figure 26: Cervical opening due to baseline change in CMP density with varying Young's Modulus values. This plots shows the effect density has on PTL.**

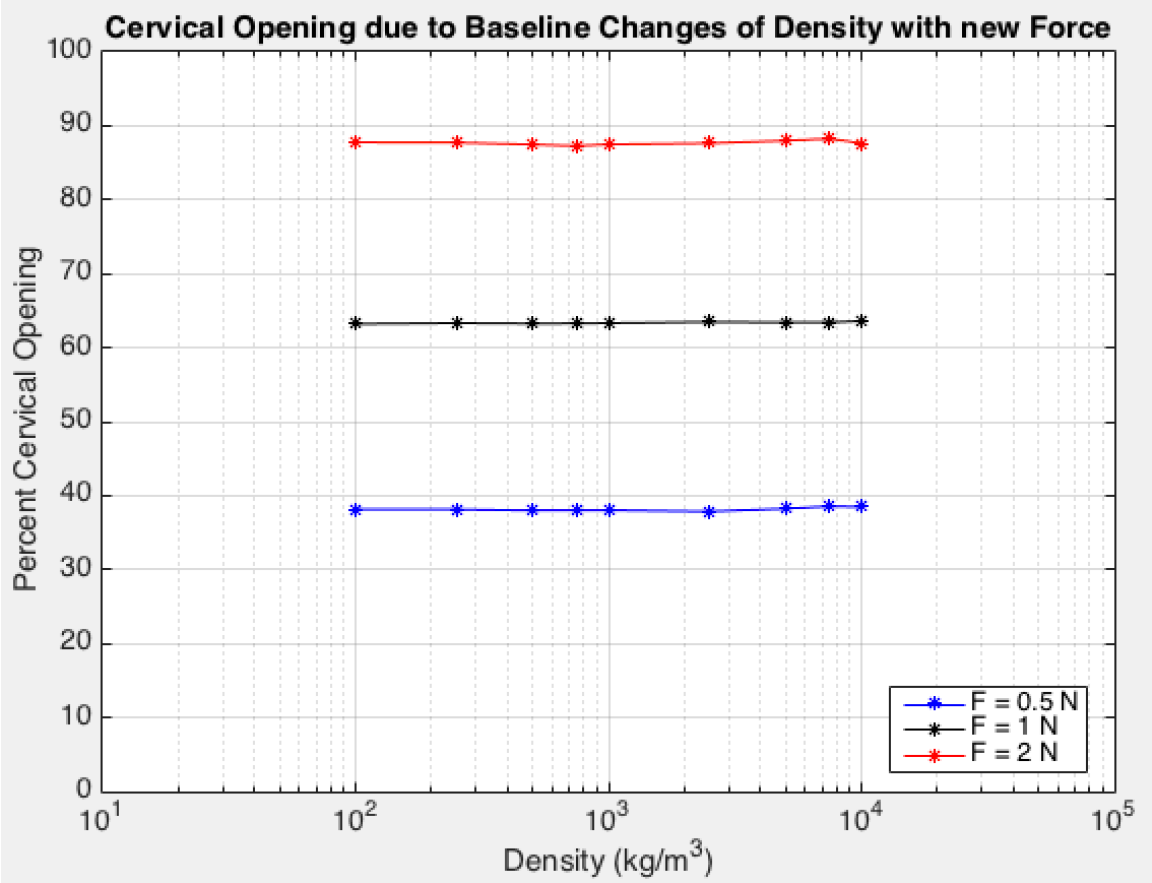


**Figure 27: Cervical opening due to baseline change in CMP density with varying force values. This plots shows the effect density has on PTL.**

Sensitivity values were then compared for each of the properties to emphasize which were the most important, as seen if Figure 28. The absolute value was taken so all the values were positive on the graph. This graph is showing the initial change from baseline values for each of the properties and it can be seen that the force and Young's Modulus were the most sensitive to changes. This supports my first hypothesis that changes in biophysical properties of the cervical tissue will affect the cervical opening. This proved my second hypothesis that changes in biophysical properties of the CMP

would affect the cervical opening to be false. Viscosity may have played a role, but it cannot be concluded whether it has a significant influence or not. Figure 28 also proves the third hypothesis that the CMP will have an important role in cervical opening to be false. However this may be due to model limitations since some of the properties could have had a greater impact if the CMP could slip along the fluid structure interface.

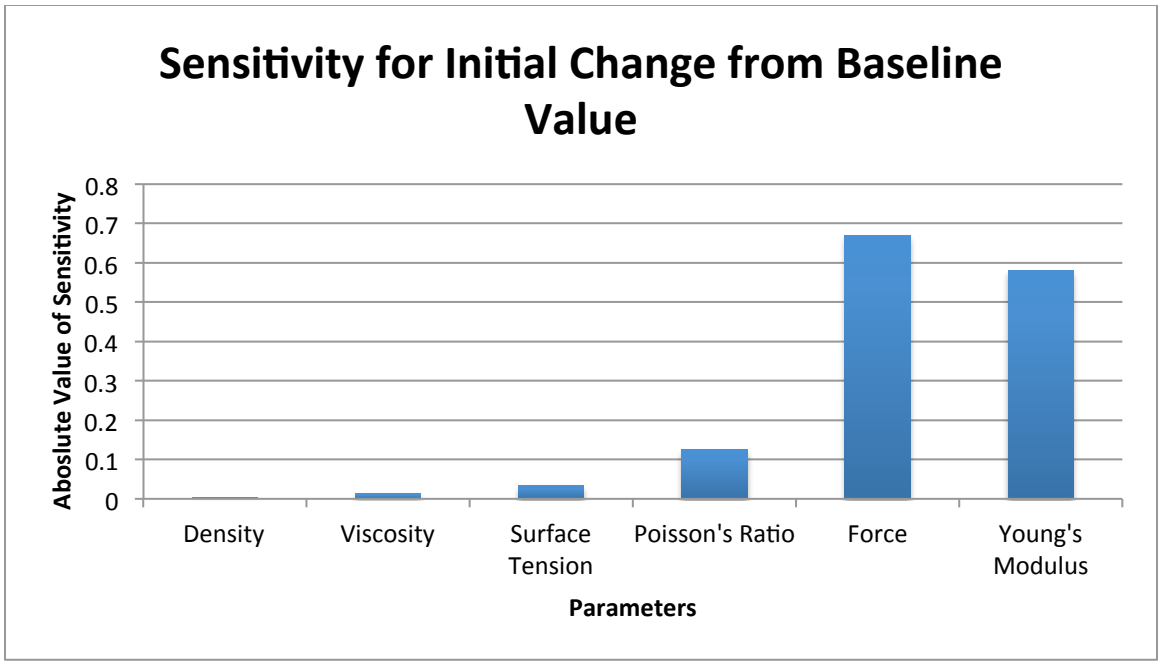


**Figure 28: Isotropic Sensitivity. This graph is showing the absolute value of the sensitivity for each parameter during the initial change from the baseline values. Young's Modulus and force can be seen to have the greatest significance in cervical opening.**

The next computation was running the model under orthotropic conditions. Looking at Figure 29, the results of the model in orthotropic conditions was compared to the isotropic version. This graph varies from the previous graphs in terms of the baseline value and the x-axis. First, the baseline value used was 0.25 kPa instead of 1 kPa and only increased since the model had errors running when the orthotropic factors became

too small. Secondly, percent cervical opening was plotted against the mean stiffness of the model instead of baseline variation. Mean stiffness was used because only one factor, whether it was R, PHI, or Z, was increased, but the overall stiffness for each computation stayed the same at each data point. Equation 33 was used to calculate the mean stiffness. $E_R$, $E_{PHI}$, and $E_Z$ represent the modulus in the R, PHI, and Z directions respectively. The isotropic line extends further since all portions of the Young's Modulus are increased, while only one is increased for the orthotropic conditions.

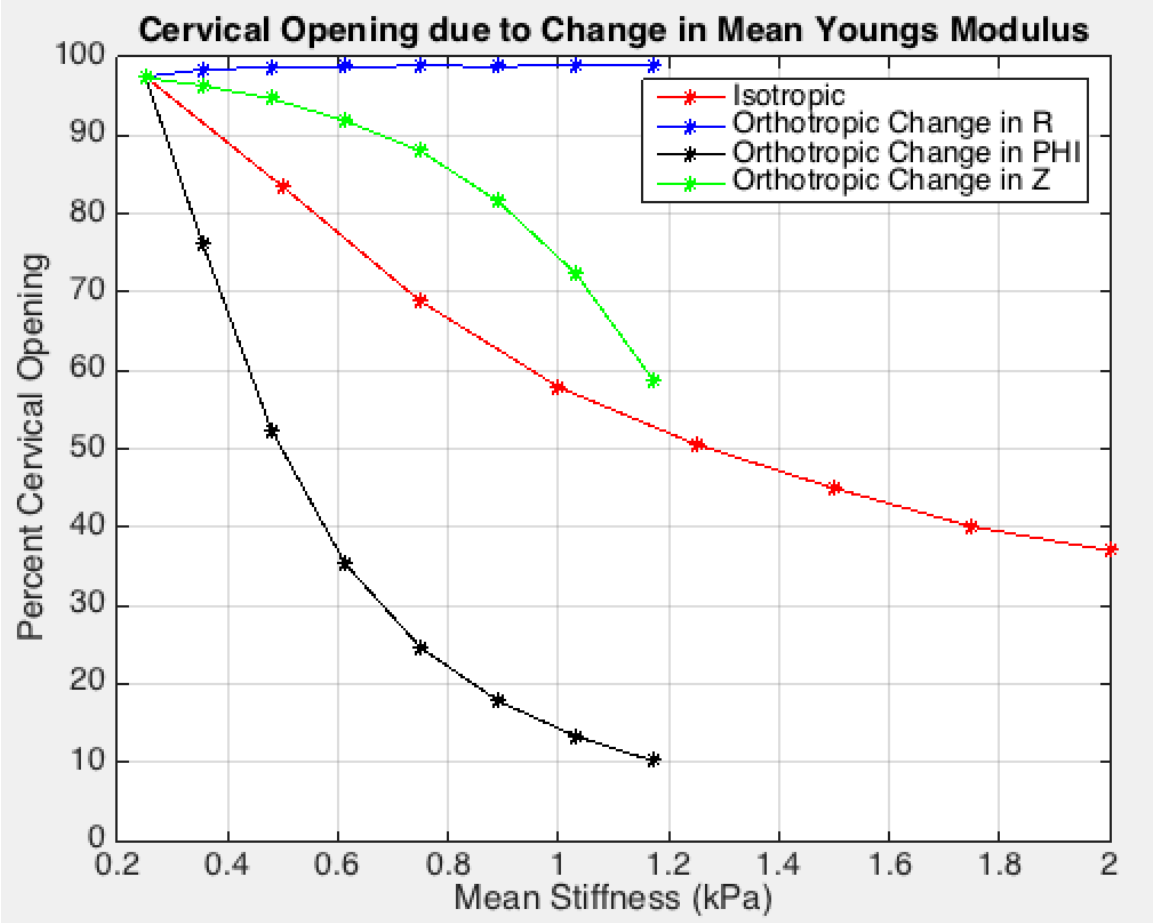


**Figure 29: Cervical opening due to changes in mean Young's Modulus. This shows the effect that the different directional forces have on percent opening in relation to each other.**

$$Mean\ Stiffness = \sqrt{\frac{E_R^2+E_{PHI}^2+E_Z^2}{3}} \quad (33)$$

Based off of the graph, the orthotropic change in R only varied slightly as the value increased from the baseline. As a result, this signified it does not have a large affect on the cervix opening. On the other hand, the orthotropic change in PHI and Z had a large effect on the percent opening. The orthotropic change in Z was not as significant as the change in PHI, but it still was influential on the system. Initially, the small values of Young's Modulus in the Z direction did not affect the percent opening to a large degree. Yet, as the value increased, the percent opening began to grow at a greater pace. The PHI direction was different since small values of Young's Modulus caused a large change in percent opening, while large values caused a smaller change. Compared to the isotropic conditions, the changes in PHI were most similar. Overall, as the cervix begins to remodel, the realignment of the fibers in the axial and circumferential directions can contribute to the cause of PTL. The circumferential direction is the most important since cervical opening decreases the most. This could potentially help to keep the cervix closed until desired to open. Additionally, other studies have shown that the circumferential direction is important. Myers created a thick-walled cylinder and displayed that the circumferential collagen fibers reduce the circumferential strain, which decreases spreading of the fibers and increases the resistance to changes in the radius of the cervix (Kristin M. Myers, Hendon, et al., 2015).

Looking at Figure 30, the results of the cervical length study can be seen. The shorter the cervix became, the higher percent cervical opening was observed. This supports previous data found, where shorter cervical length is a high risk factor leading to PTL. There is a linear trend in the opening of the cervix, but each decrease in size cause a large amount of percent opening. This supports the fourth hypothesis that the model will verify that cervical length is important. Understanding the size of the person's cervix is critical in protecting the woman from entering PTL. It is also interesting to see that with this model, the cervical length did not have as large of an impact as cervical stiffness did. Looking at Figure 17, the percent cervical opening went from 10 to 100 percent for cervical stiffness, while only going from around 60 to about 95 percent for cervical length.

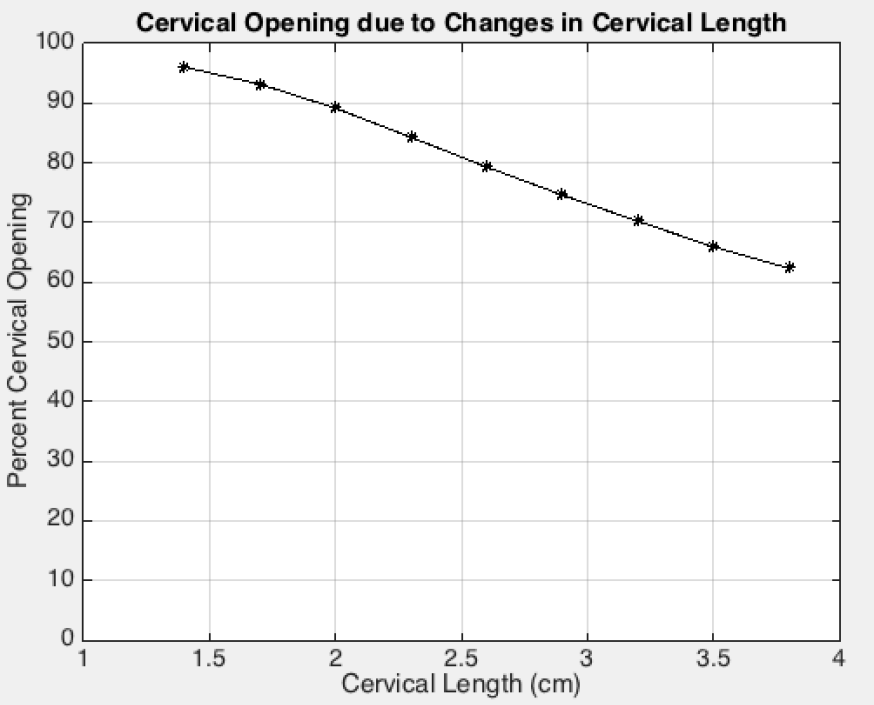


**Figure 30: Cervical length study. This shows how different cervical lengths affect the percent opening of the cervix.**

Since a short cervix proved to be an influential indicator of leading to PTL, the parameters were varied individually with a cervix length of 1.7 cm. The variation was done in order to see the effect that the parameters have when the cervix is short. Sensitivity calculations were then performed again for the shorter cervix and compared to the normal cervix. Based on Figure 31, as the cervix gets smaller, the CMP properties seemed to have more significance and may play a larger role. This shows that although the CMP is not important for a normal cervix, it could be critical to monitor with a short cervix.

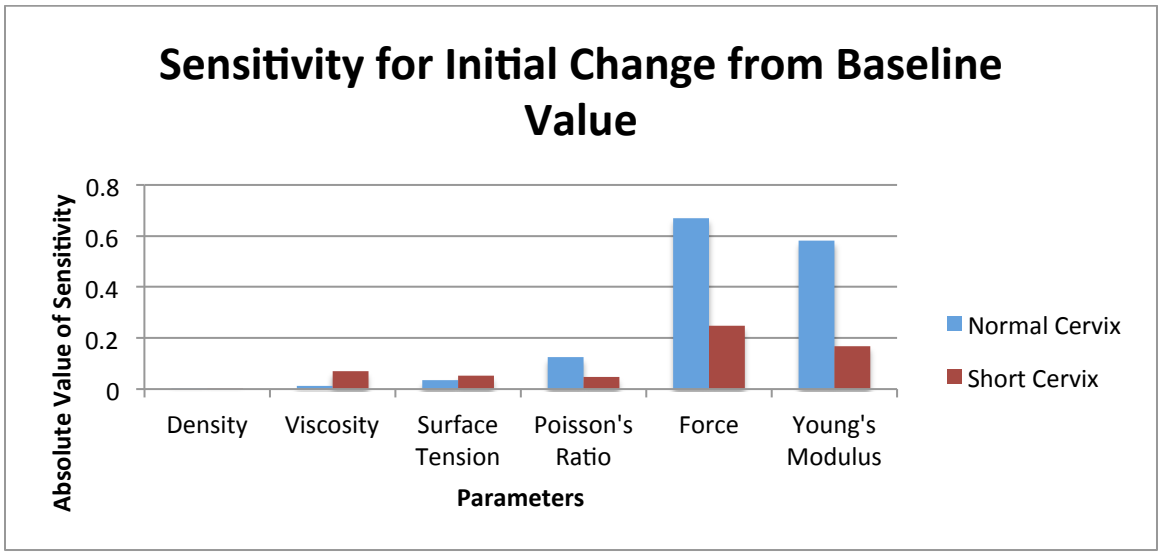


**Figure 31: Sensitivity comparison for a normal and short cervix. The short cervix sensitivities were closer for the cervical tissue and the CMP that indicates the CMP may play a larger role in preventing PTL.**

The impact of surface tension with a short cervix can be seen in Figure 32. Surface tension had a slightly larger influence on the system, but the results were once again surprising. They were surprising because the higher surface tension actually caused the cervix to open more. If anything, it was expected that the surface tension would cause

lesser opening at greater values. The results may be due to the limitation that the CMP could not slip in the model. Similarly from Figure 33, viscosity seemed to be more important to the system. The trends of the viscosity for the short and normal cervix were slightly different, where the normal cervix causes lesser opening below baseline values, while the short cervix caused greater opening below baseline values. Despite the trend difference, viscosity still had a larger role as the cervix size became smaller. As a result, this may need to be monitored by doctors when evaluating a woman for risk of PTL.

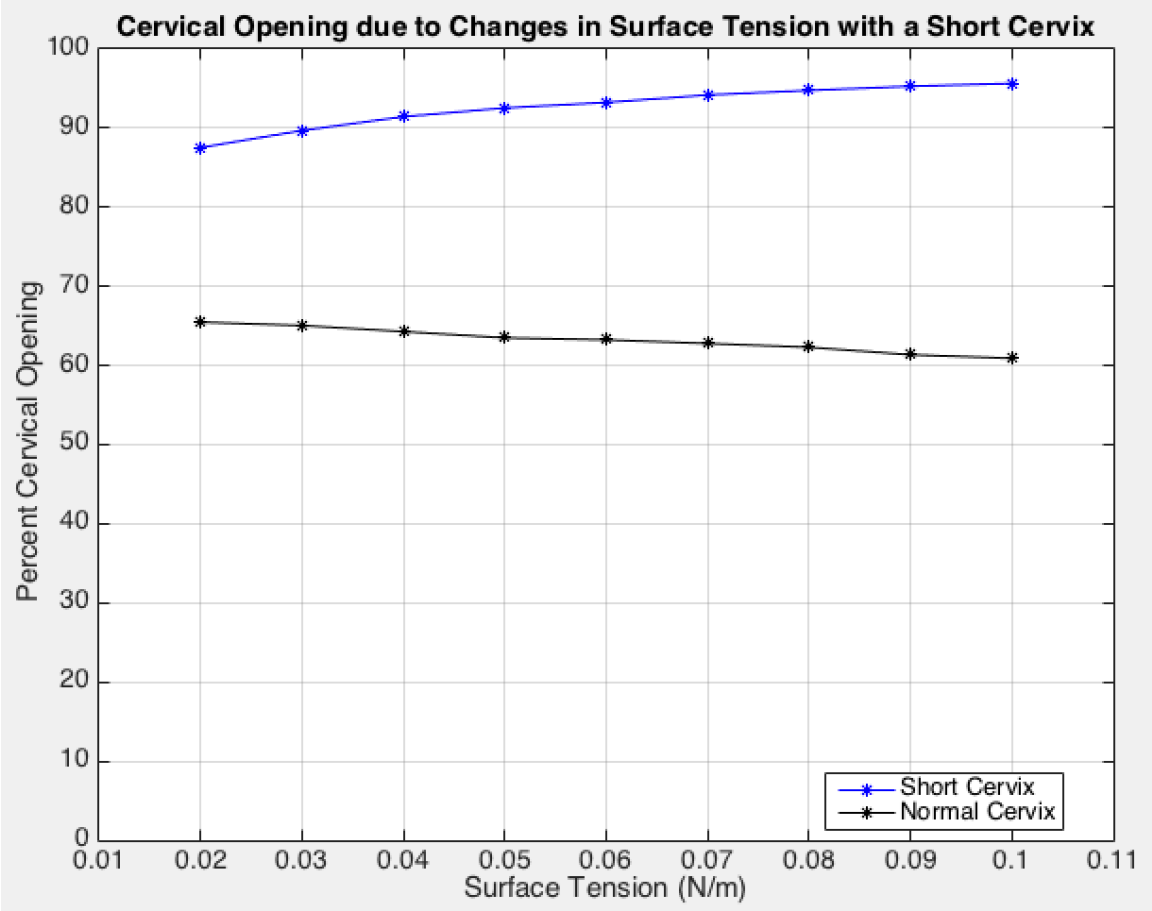


**Figure 32: Cervical opening due to baseline changes in surface tension with a short cervix. The surface tension of the short cervix has a greater impact on cervical opening than the normal cervix.**

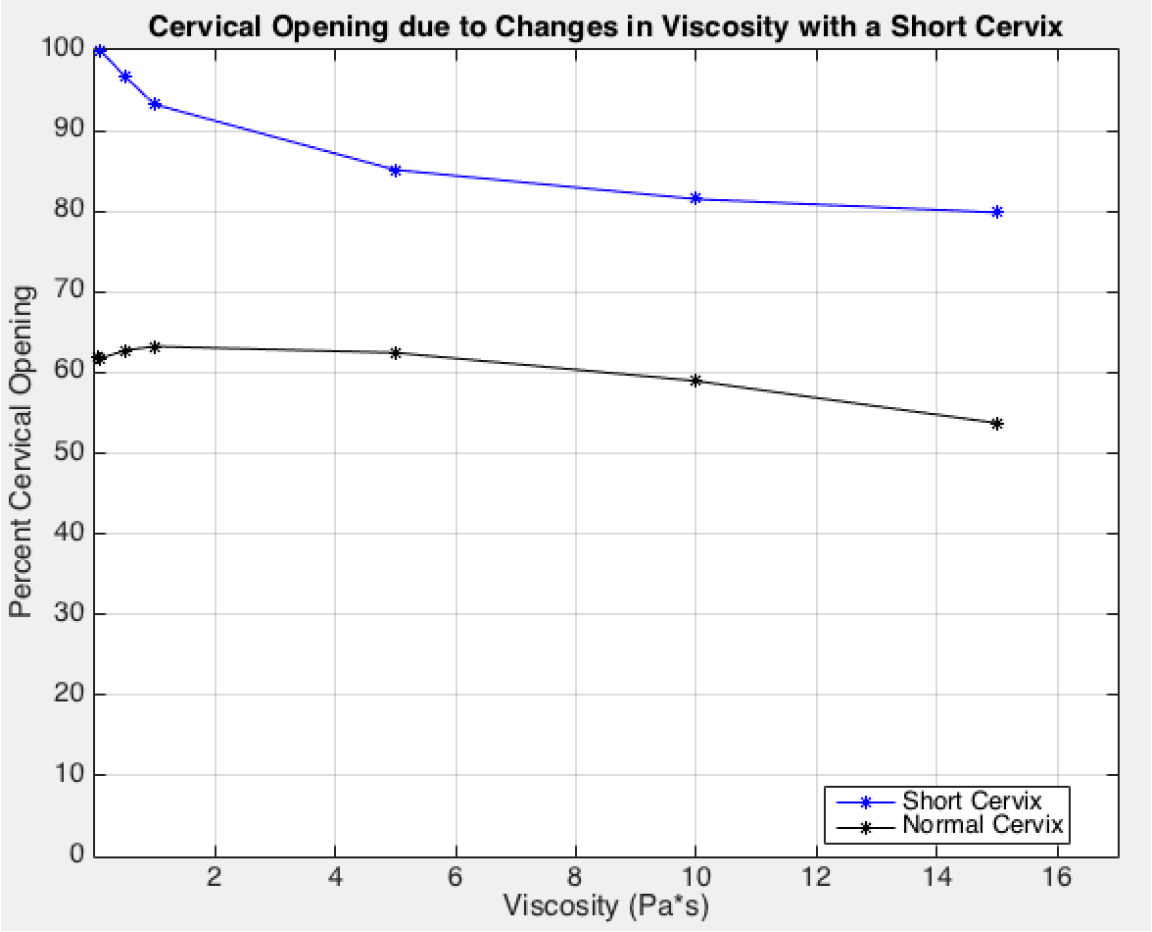


**Figure 33: Cervical opening due to baseline changes in viscosity with a short cervix. The viscosity of the short cervix has a greater impact on cervical opening than the normal cervix.**

# CHAPTER 4: CONCLUSION

The main goal of this project was to create computational models of the cervix remodeling during PTL to determine the factors that could cause PTL. An axial symmetric model was created to show the influence of biomarkers of the CMP and the cervical tissue in relation to PTL. Mechanical properties of the CMP and the cervical tissue were tested and plotted in order to determine their impact on the system. For the CMP, the factors that were focused on were viscosity, surface tension, and density. Likewise, for the cervical tissue, the factors tested were Poisson's Ratio, force, and Young's Modulus. The model was run in both isotropic and orthotropic conditions to test certain factors.

Overall, the model created was very simplistic, but multiple factors could be measured. Understanding that the cervix tissue is more important than the CMP helps to know where prevention techniques should be focused on. Additionally, the cervical length results found showed the model was good enough to match previous data in other studies. This is a well know issue and the model was able to support it. Despite the simple concept of the model, it still provided good insight on the biophysical factors that could affect cervical opening

After tests were completed, it was found that the Young's Modulus and force played a significant role in the remodeling of the cervix during PTL. This proved the hypothesis that the cervical tissue biophysical properties will cause changes to be true. The only factor that started to play a role for the CMP at high values was viscosity and cannot be ruled out as not having an important part in preventing PTL. Similarly, the

surface tension may have played a larger role had there not been limitations with the model. Yet, it was inconclusive whether these were important so it did not support prove the hypothesis that the biophysical properties of the CMP would cause changes to cervical opening. The structure of the CMP as a whole did not have as large of an influence on the system as hypothesized. The main hypothesis that was looked at was if the influence of the overall structure of the CMP would be important in predicting PTL and based off of the results, it proved the hypothesis to be false.

Once the Young's Modulus was determined as an important factor, it was run in orthotropic conditions to see if fiber alignment had an effect. As seen in the plots, the fiber alignment in the axial and circumferential directions affected the opening of the cervix. The circumferential direction should especially be made aware of because it resists the opening of the cervix. If this can be made stronger, PTL may be able to be prevented from occurring. Based off of this information, the model suggests that doctors should be aware of the stiffness of the cervix in these specific directions. Understanding that cervical tissue may be important could help to allow the baby to keep developing and would reduce death and disabilities that result from premature birth.

Another important factor that must be focused on is the cervical length. Based off of the data found and previous studies, shorter cervical lengths caused a greater percent opening for the cervix. This proved the last hypothesis to be correct that the model would verify cervical length is important. As a result, physicians must measure the length of the cervix early in the process to determine the potential risk for their patients. If a shorter cervix is found doctor appoints should potentially occur more regularly in order to

monitor the cervix and keep the opening under control. Providing ways to establish a greater stiffness could hypothetically counter the short cervix to prevent PTL as long as possible. Similarly, the CMP may play a larger role with a shorter cervix. Referring to the main hypothesis, this began to support it and the CMP structure as whole may need to be monitored in the situations where a patient has a shorter cervix.

There is one large improvement to the system that could be made in order to get more accurate results. The improvement would be to find a way to allow the CMP to slip along the shared boundary with the cervical tissue, as seen in Figure 24. If this process could be factored into the model, the CMP's significance for the system may change. Surface tension especially would be expected to play a larger role since it would be adjusted as the plug shape changes. With the CMP potentially having a more important role, it would be imperative to keep the CMP from shedding for as long as possible.

The next step for the system would be to create a more advanced model. Currently, the model only represents the cervical tissue and the CMP operating in dilation. Adjusting boundary conditions so that effacement could be included would be important. If a new model was created with the uterus as well, as in Figure 34, more accurate forces could be placed and the significant factors may change. The model could be computed at different uterus sizes, depending on the time during the gestation period, or it could grow to reach a certain time point in the gestation period. With this new model, the forces would be applied upon all of the inner walls of the uterus and the cervix and on the top of the CMP. Values of the intrauterine pressure would range from 0 to 13 kPa, where 8.6 kPa is the peak intrauterine pressure during uterine contraction

(Fernandez et al., 2016). This would be more similar to the pressures that a baby would apply on the system and it could help to solidify the results found from the model used in this study. Another step that could be taken would be to change the viscosity of the fluid to a non-Newtonian viscosity instead of a Newtonian one. Normally, the viscosity is a non-Newtonian shear thinning fluid (Lai et al., 2009). Important ranges are from $10^{-1}$ to $10^{0.5}$ Pa*s and the viscosity should be varied between these (Lai et al., 2009). The viscosity of the CMP changes with the menstruation cycle and this may occur during the gestation period as well. The viscosity is a non-linear fluid and the shear dependence of it may be important in cervical opening.

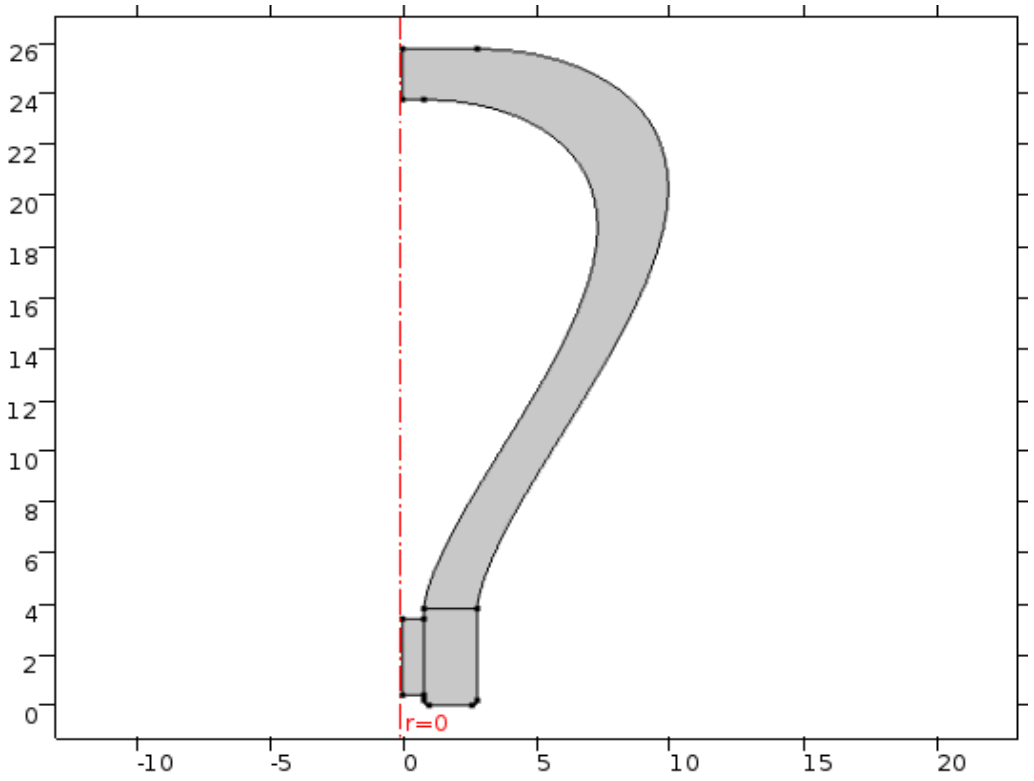


**Figure 34: Cervix with the uterus included. This is a more anatomically accurate representation of the reproductive system and could produce improved results.**

REFERENCES

Baah-Dwomoh, A., McGuire, J., Tan, T., & De Vita, R. (2016). Mechanical Properties of Female Reproductive Organs and Supporting Connective Tissues: A Review of the Current State of Knowledge. *Applied Mechanics Reviews*, *68*(6), 60801-60801–12. https://doi.org/10.1115/1.4034442

Bastholm, S. K., Becher, N., Stubbe, P. R., Chronakis, I. S., & Uldbjerg, N. (2014). The viscoelastic properties of the cervical mucus plug. *Acta Obstetricia Et Gynecologica Scandinavica*, *93*(2), 201–208.

Becher, N., Adams Waldorf, K., Hein, M., & Uldbjerg, N. (2009). The cervical mucus plug: structured review of the literature. *Acta Obstetricia Et Gynecologica Scandinavica*, *88*(5), 502–513. https://doi.org/10.1080/00016340902852898

Cervical Dilation | Pregnancy Delivery | labor and Child Delivery :: Mothersspace. (n.d.). Retrieved February 22, 2017, from http://www.mothersspace.in/giving-birth/all-about-labour/cervical-dilation/

Critchfield, A. S., Yao, G., Jaishankar, A., Friedlander, R. S., Lieleg, O., Doyle, P. S., … Ribbeck, K. (2013). Cervical Mucus Properties Stratify Risk for Preterm Birth. *PLOS ONE*, *8*(8), e69528. https://doi.org/10.1371/journal.pone.0069528

Fernandez, M., House, M., Jambawalikar, S., Zork, N., Vink, J., Wapner, R., & Myers, K. (2016). Investigating the mechanical function of the cervix during pregnancy using finite element models derived from high-resolution 3D MRI. *Computer Methods in Biomechanics and Biomedical Engineering*, *19*(4), 404–417. https://doi.org/10.1080/10255842.2015.1033163

Goldenberg, R. L., Culhane, J. F., Iams, J. D., & Romero, R. (2008). Epidemiology and causes of preterm birth. *The Lancet*, *371*(9606), 75–84. https://doi.org/10.1016/S0140-6736(08)60074-4

Hein, M., Helmig, R. B., Schønheyder, H. C., Ganz, T., & Uldbjerg, N. (2001). An in vitro study of antibacterial properties of the cervical mucus plug in pregnancy. *American Journal of Obstetrics and Gynecology*, *185*(3), 586–592. https://doi.org/10.1067/mob.2001.116685

House, M., Kaplan, D. L., & Socrate, S. (2009). Relationships Between Mechanical Properties and Extracellular Matrix Constituents of the Cervical Stroma During Pregnancy. *Seminars in Perinatology*, *33*(5), 300–307. https://doi.org/10.1053/j.semperi.2009.06.002

Huddy, C., Johnson, A., & Hope, P. (2001). Educational and behavioural problems in babies of 32-35 weeks gestation. *Archives of Disease in Childhood. Fetal and Neonatal Edition*, *85*(1), F23–F28. https://doi.org/10.1136/fn.85.1.F23

Jung, E. Y., Park, J. W., Ryu, A., Lee, S. Y., Cho, S., & Park, K. H. (2016). Prediction of impending preterm delivery based on sonographic cervical length and different cytokine levels in cervicovaginal fluid in preterm labor. *JOG Journal of Obstetrics and Gynaecology Research*, *42*(2), 158–165.

Lai, S. K., Wang, Y.-Y., Wirtz, D., & Hanes, J. (2009). Micro- and macrorheology of mucus. *Advanced Drug Delivery Reviews*, *61*(2), 86–100. https://doi.org/10.1016/j.addr.2008.09.012

Mazaki-Tovi, S., Romero, R., Kusanovic, J. P., Erez, O., Pineles, B. L., Gotsch, F., … Than, N. G. (2007). Recurrent Preterm Birth. *Seminars in Perinatology*, *31*(3), 142–158. https://doi.org/10.1053/j.semperi.2007.04.001

Myers, K. M., Feltovich, H., Mazza, E., Vink, J., Bajka, M., Wapner, R. J., … House, M. (2015). The mechanical role of the cervix in pregnancy. *Journal of Biomechanics*, *48*(9), 1511–1523. https://doi.org/10.1016/j.jbiomech.2015.02.065

Myers, K. M., Hendon, C. P., Gan, Y., Yao, W., Yoshida, K., Fernandez, M., … Wapner, R. J. (2015). A continuous fiber distribution material model for human cervical tissue. *Journal of Biomechanics*, *48*(9), 1533–1540. https://doi.org/10.1016/j.jbiomech.2015.02.060

Myers, K. M., Paskaleva, A. P., House, M., & Socrate, S. (2008). Mechanical and biochemical properties of human cervical tissue. *Acta Biomaterialia*, *4*(1), 104–116. https://doi.org/10.1016/j.actbio.2007.04.009

Myers, K. M., Socrate, S., Paskaleva, A., & House, M. (2010). A Study of the Anisotropy and Tension/Compression Behavior of Human Cervical Tissue. *Journal of Biomechanical Engineering*, *132*(2), 21003-21003–15. https://doi.org/10.1115/1.3197847

RN, W. D. (n.d.). Vitals and Bits #6: The Cervix. Retrieved February 22, 2017, from http://alibi.com/blog/s/health/32688/story.html

Short_cerix.jpg (301×225). (n.d.). Retrieved February 23, 2017, from http://www.marchofdimes.org/glue/css-images/_notes/Short_cerix.jpg

Singh A.K, & Bhadauria B.S. (2009). Finite difference formulae for unequal sub-intervals using Lagrange's interpolation formula. *Int. J. Math. Anal. International Journal of Mathematical Analysis*, *3*(17–20), 815–827.

van Baaren, G.-J., Vis, J. Y., Wilms, F. F., Oudijk, M. A., Kwee, A., Porath, M. M., … Mol, B. W. J. (2014). Predictive value of cervical length measurement and fibronectin testing in threatened preterm labor. *Obstetrics and Gynecology*, *123*(6), 1185–1192. https://doi.org/10.1097/AOG.0000000000000229